THE UNIVERSITY OF MANITOBA

GRAIN SIZE EFFECT ON LOW CYCLE FATIGUE BEHAVIOR OF COPPER POLYCRYSTALS

By

Wei Liu

A thesis
submitted to the faculty of graduate studies
in partial fulfillment of the
requirements for the degree of
Master of Science

DEPARTMENT OF MECHANICAL AND INDUSTRIAL ENGINEERING
WINNIPEG, MANITOBA
JANUARY 2000

THE UNIVERSITY OF MANITOBA

FACULTY OF GRADUATE STUDIES

*****

COPYRIGHT PERMISSION PAGE

Grain Size Effect on Low Cycle Fatigue Behavior of Copper Polycrystals

BY

Wei Liu

A Thesis/Practicum submitted to the Faculty of Graduate Studies of The University of Manitoba in partial fulfillment of the requirements of the degree of Master of Science

ACKNOWLEDGMENTS

This project is the final result of over two years of work, collaboration and especially the establishment of so many excellent friends, who made my stay at the university of Manitoba one of the most pleasant experiences of my life.

I would like to express my most sincere gratitude to my advisor: Professor M. Nabil Bassim for his outstanding advice, encouragement and understanding throughout this project. It has been of great educational and real-life value to have worked under his supervision.

My appreciation is also extended to Mr. Don Mardis, Mr. John Van Dorp and Mr. Irwin Penner for instructing me on using research facilities. I would also thank to my friends: H. Feng, Q. Xu, H. W. Guo, N. Panic, M. Aezeden, U. Prasad and C. Iyer for their help and motivation. My special thanks are to my parent for their constant encouragement and moral support.

TABLE OF CONTENTS

LIST OF FIGURES

LIST OF TABLES

LIST OF SYMBOLS

ε_a	strain amplitude
$\Delta\varepsilon$	total strain amplitude
$\Delta\varepsilon_{pl}$	total plastic strain
$\Delta\varepsilon_{pl}/2$	plastic strain amplitude
$\Delta\varepsilon_e$	total elastic strain
σ_a	stress amplitude
$\Delta\sigma$	total stress amplitude
$\Delta\sigma_s$	total saturation stress
$\Delta\sigma_s/2$	saturation stress amplitude
M	effective orientation factor
f_m	volume fraction of matrix structure
f_{PSB}	volume fraction of PSB structure
τ_m	shear stress in matrix structure
τ_{PSB}	shear stress in PSB structure
f_{PSB}	the volume fraction of the PSBs
e_b	local plastic shear strain amplitude in the ladder structure
e_m	the local plastic shear strain amplitude in the matrix structure

$\Delta\gamma_{pl}/2$	the plastic shear strain amplitude applied.
E	modulus of elasticity
A	cross-section area of the test section of the specimen
F	load applied to the specimen
HRF	Rockwell hardness F scale
SEM	scanning electron microscope
CSSC	cyclic stress-strain curve
PSBs	persistent slip bands
SSBs	secondary slip bands

ABSTRACT

Cyclic deformation of polycrystalline copper has been studied for two decades. However, the reported results are quite controversial over the plateau behavior, which has been well established for copper single crystals. The absence of complete and reliable results on the effects of the grain size on the cyclic behavior for polycrystalline copper determines the main objective of the present study, which was conducted in an attempt to address the reason for the existing scatter in the literature.

The grain size effect on low cycle fatigue (LCF) behavior of copper polycrystals was studied at room temperature under symmetric tension-compression cycling at constant total strain amplitude control with a low constant plastic strain rate. Sets of specimens with different grain sizes were cyclically tested, over a range of plastic strain from 5×10^{-6} to 5×10^{-3}, up to saturation. The obtained saturation stresses were plotted as a function of corresponding plastic strain amplitudes to obtain a cyclic stress strain curve (CSSC) for each grain size. Finally, all the cycled specimens were sectioned and cut longitudinally in the mid-section of the specimens to produce samples for microscopic investigation. Scanning electron microscopy (SEM) was conducted on the etched samples for the evidence of persistent slip bands (PSBs).

Investigation of the influence of grain size on the cyclic response of 22μm-, 35μm- and 100μm-grained copper polycrystals exhibits strong differences, although all of them exhibit three regions of cyclic hardening in common. Except at very low plastic

amplitude, where difference in saturation stress is unclear, smaller-grained polycrystals exhibit higher stress value over the range of the plastic amplitude at which the LCF was conducted. A tendency of interception of the CSS curves at high plastic amplitude suggests that grain size might lose effect at higher plastic strain. The obtained CSS curves all reveal quasi-plateau behaviors. However, the quasi-plateaus for different-grained materials show difference in slope, location and extension. SEM investigation indicates grain size effect on occurrence of PSBs in amount, rate and location, which determine the different characteristics of quasi-plateau regions for different grain sizes.

The obtained cyclic properties and observed microstructure development were correlated by introducing a realistic grain model and explained in light of previous work by M. N. Bassim and C. D. Liu at the University of Manitoba.

CHAPTER 1: INTRODUCTION

Fatigue is the failure phenomenon of a material under cyclic loading and deformation. Under a repeatedly applied cyclic deformation, fracture is produced by strain amplitude that is far below the strain associated with fracture under a monotonic loading. Fatigue is a major cause of failure of structures and components and is becoming more and more critical due to increasing demand for high strength materials and the introduction of new materials whose mechanical response is not well understood.

Over the later part of the present century, the work on fatigue has covered the fracture aspects, i.e., crack propagation and fracture mechanics. This research has been extremely valuable in diagnostics, failure analysis and in the fracture control of structures. However much of this work has been carried out from an engineering point of view and less attention has been given to the basic mechanisms of fatigue. It is recognized that without a fundamental understanding of such basic processes, designing structures with higher safety would be difficult.

The fatigue process is completely dominated by cyclic plastic deformation, which causes irreversible changes in the material microstructure. In general, the fatigue process can be divided into three stages: fatigue hardening and/or softening, microcrack nucleation, and crack propagation [1]. The final stage has received the most attention and can be considered to be well established. On the other hand, the first two stages, where most of the fatigue problems in many types of structure, have received less attention and there are still a lot of unsolved problems.

During the last three decades a group of workers in the research community has started to approach the fatigue problem from a different point of view and has established the new field of cyclic deformation. In this field, the dislocation behavior and the mechanism of cyclic deformation, including the role of microstructure in controlling cyclic stress-strain response, have been studied, focusing especially on the early stages, which are critical for predicting fatigue life of materials.

Since early 70s there have been a number of studies dealing with the cyclic stress-strain behavior of pure metals and alloys. Most of them were on single crystals because it is helpful to understand basic fatigue behavior. Throughout those investigations understanding of phenomena, such as cyclic response and corresponding mechanism, has been achieved. Over the past two decades the cyclic deformation behavior of polycrystalline materials has also been studied. However, investigations have given rise to a considerable scatter in the reported results. In order to provide some answers to the understanding of the behavior of material under cyclic deformation, the present study investigates the grain size effect on low cycle fatigue behavior of polycrystalline copper.

Chapter 2: LITERATURE REVIEW

This chapter reviews major features of the cyclic deformation of copper single and polycrystals that were reported in the literature. The influence of parameters such as testing mode, testing frequencies or strain rates and grain size on the cyclic response, strain localization and the associated dislocation structures of copper, are provided.

2.1 CYCLIC DEFORMATION OF COPPER SINGLE CRYSTAL

Under application of cyclic load or strain, an annealed single crystal shows an initial period of cyclic hardening, followed by softening, and finally a steady state of deformation referred to as cyclic saturation [2-9]. The phenomenon of saturation is due to reversible processes involving defect production and annihilation. The saturation values of stress or strain depend on the particular applied plastic strain or stress amplitudes respectively, and used to define the cyclic stress-strain curve (CSSC). The final stages of cycling include fatigue crack initiation, propagation and the final failure.

The CSS curve of copper single crystal is well-known for having three clearly defined regions as given in Figure 2.1. The three regions are directly related to different dislocation arrangements and therefore different hardening behaviors.

The first region, A ($\Delta\varepsilon_{pl}/2 < 6\times10^{-5}$), is a rapid hardening stage and has been shown to be due to accumulation of edge dislocation dipoles. At very low amplitudes, the basic

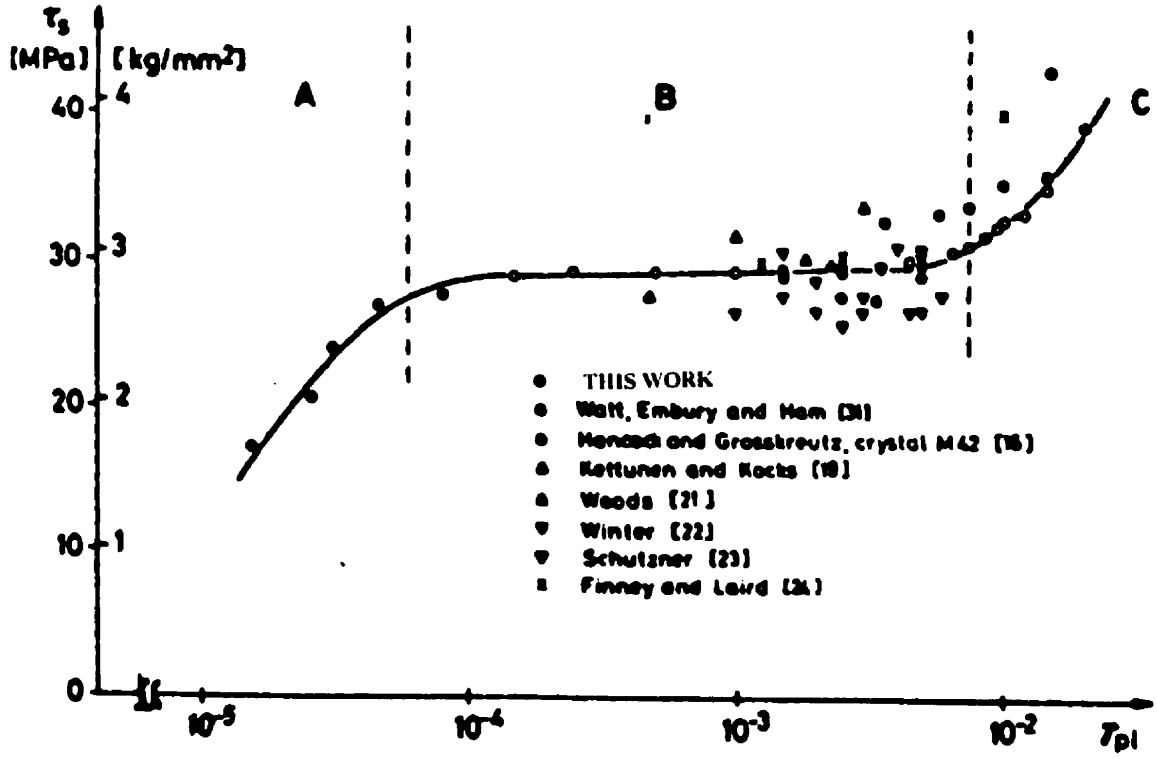

Figure 2.1 CSSC of copper single crystal at constant strain amplitude, from Ref. [8]

element of the dislocation structures consists of dipole bundles, which have been named unit loop patches [10]. At higher amplitudes, larger loop patches of primary edge dislocations (Fig.2.2a) are the characteristic dislocation arrangement for the whole range and are known as matrix structure. Higher plastic deformation, within the region, causes a denser matrix structure and higher saturation stresses.

At plastic strain amplitudes above 6×10^{-5}, the saturation stress is constant over a wide range. This intermediate region B is called plateau stage and extends up to plastic strain amplitudes of 7.5×10^{-3}. The onset of the plateau is marked by the formation of persistent slip bands (PSBs). After PSB formation, the deformation is no longer homogeneous, and the matrix structure breaks down locally into the well-known ladder structure of the PSBs (Fig. 2.2b), which behave as channels where large amounts of strain are concentrated [11-15]. As the strain amplitude increases along the plateau, the PSB volume fraction increases linearly up to shear strain of 7.5×10^{-3}(Figure 2.3), where the specimen is filled completely with PSBs (2.2c). In plateau region, the saturation stress, which is mainly governed by the PSBs, remains almost constant.

In region C, the saturation stress increases with increasing plastic strain amplitude. Occurrence of work hardening in the specimens filled entirely with PSBs is related to new structural changes in the dislocation arrangements. The deformation becomes more homogeneous and a mixed wall-cell structure (Fig. 2.2d) is observed, which is characterized by increasing amounts of secondary slip (enhanced multiple slip) and decreasing wall spacing as shear strain amplitude is increased.

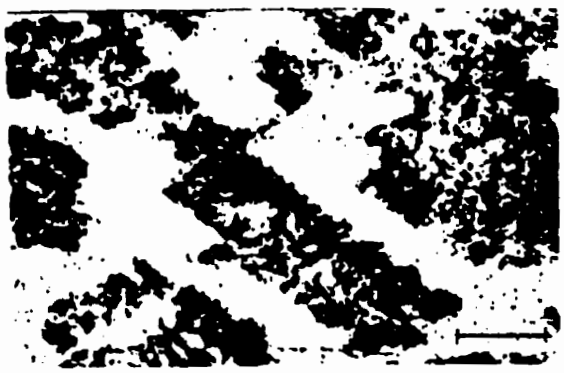

a) Range A : $\gamma_{pl} < 6 \times 10^{-5}$.
Primary dipole veins.

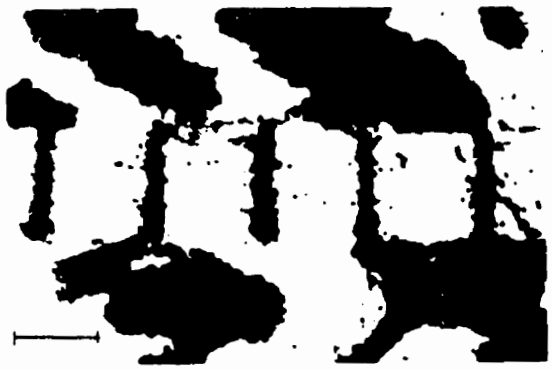

b) Range B : $6 \times 10^{-5} < \gamma_{pl} < 7.5 \times 10^{-}$
Primary dipolar walls of PSBs in matrix of primary dipole veins.

b_p

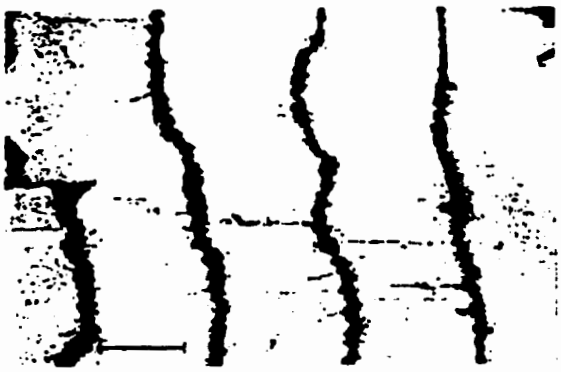

c) End of plateau : $\gamma_{pl} = 7.5 \times 10^{-3}$.
Primary dipole walls.

d) Range C : $\gamma_{pl} > 7.5 \times 10^{-3}$.
Secondary dipole walls and cells.

Figure 2.2 Dislocation evolution in copper single crystal, from Ref. [8]

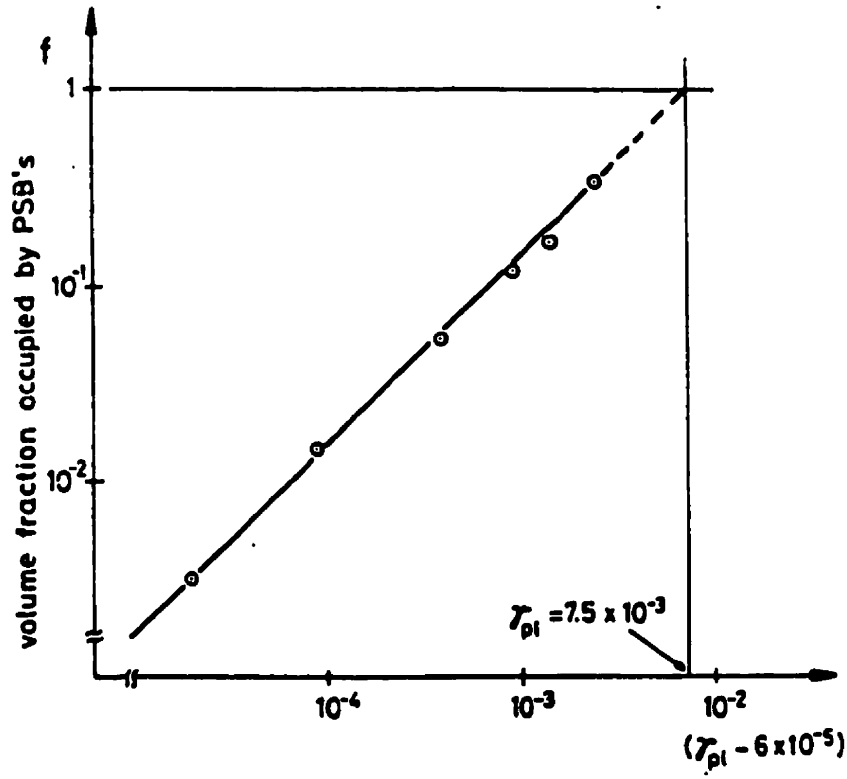

Figure 2.3 Volume fraction of PSBs as a function of plastic strain amplitude in copper single crystals, from Ref. [8]

2.2 CYCLIC DEFORMATION OF COPPER POLYCRYSTALS

During the last two decades, cyclic deformation of copper polycrystals has been studied extensively [16- 40]. However, investigations into the CSSCs of copper polycrystals have given rise to a considerable scatter in the reported results. The scatter has arisen over whether or not the CSSCs for copper polycrystals can be correlated with that for copper single crystal. The main controversy concentrates on whether or not there is a plateau in the CSSC of copper polycrystals. There are many factors that could be considered as possible causes for this scatter such as testing mode, microstructure, strain rate of testing, chemical composition and previous history. Thus, in this section, the previous work will be reviewed not only on results but also on the test conditions including the above mentioned factors.

2.2.1 Cyclic stress-strain curves (C.S.S.C) in copper polycrystals

It is well established that there exists a plateau region in cyclic stress-strain curve for copper single crystal. In the past two decades, studies on the understanding of cyclic response in copper polycrystals were carried out to compare with that of single crystal, especially in the plateau region. There has been a controversy about the existence of such a stage in the C.S.S.C of polycrystalline copper.

2.2.1.1 Plateau behavior in copper polycrystals

Rasmussen and Pedersen [17] claimed a plateau in copper polycrystals fatigued in tension-compression at room temperature. The polycrystals tested had a grain size of 150μm. The test was performed under constant strain amplitude control. A frequency of 0.25Hz was kept constant throughout the entire test. Figure 2.4 shows the C.S.S.C obtained from his study. For comparison, a C.S.S.C for single crystal was also given. They concluded that both monocrystalline and polycrystalline copper showed a plateau, although the plateau for the polycrystals extended to plastic shear strain amplitude of only 10^{-3}, which is lower than the value of 7.5×10^{-3} for the single crystal.

Figueroa *et al.* [18] studied the cyclic response of copper polycrystals under conventional strain and load control tests, where a constant frequency of 10Hz was used in the plastic range from 10^{-5} to 10^{-2}. They reported that strain control curve did not show a true plateau. However, as can be seen in Figure 2.5, the stress control C.S.S.C tends strongly to a plateau (at about 70Mpa).

Kuokkala *et al.* [20] claimed a very horizontal plateau in his study in 2mm-grained specimens tested under constant plastic strain control. Figure 2.6 shows the C.S.S.C obtained in the study, it can been seen that the plateau extends through a range of plastic shear strain amplitudes from 4×10^{-4} to 10^{-3}, which is shorter than that of copper monocrystal.

2.2.1.2 Plateau-like behavior in copper polycrystals

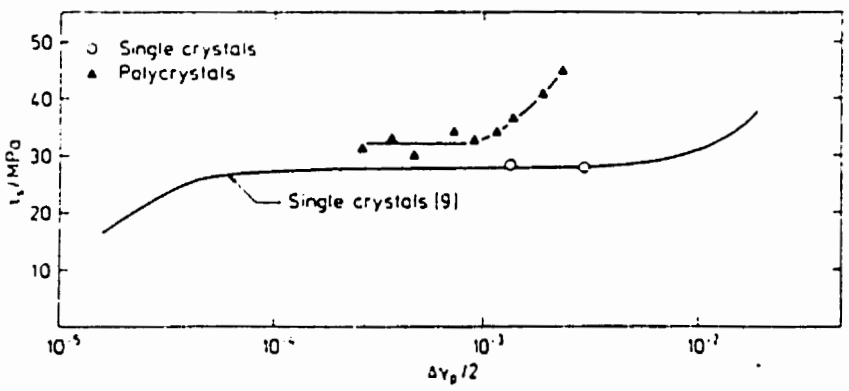

Figure 2.4 CSSC for 150μm-grained copper tested under constant strain amplitude control with a constant low frequency, from Ref. [17]

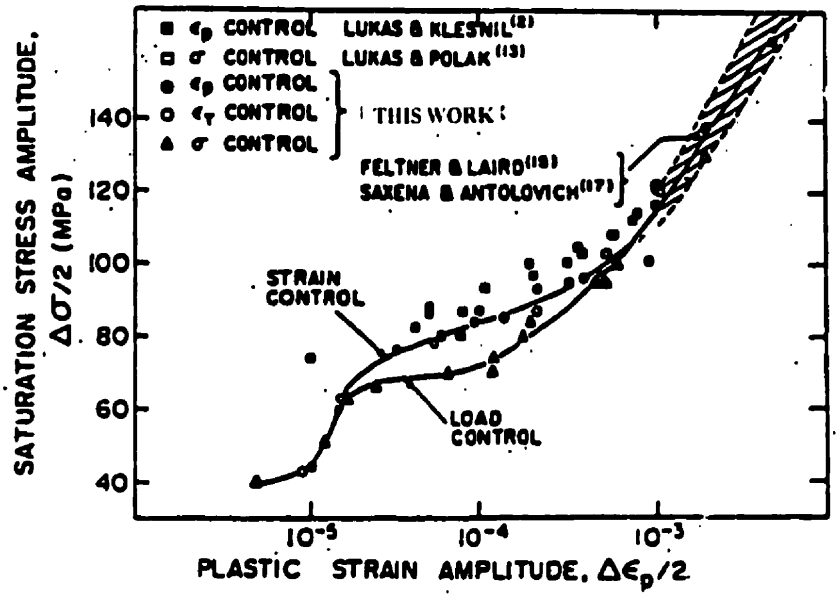

Figure 2.5 CSSC for copper polycrystals under various modes of control, from Ref. [18]

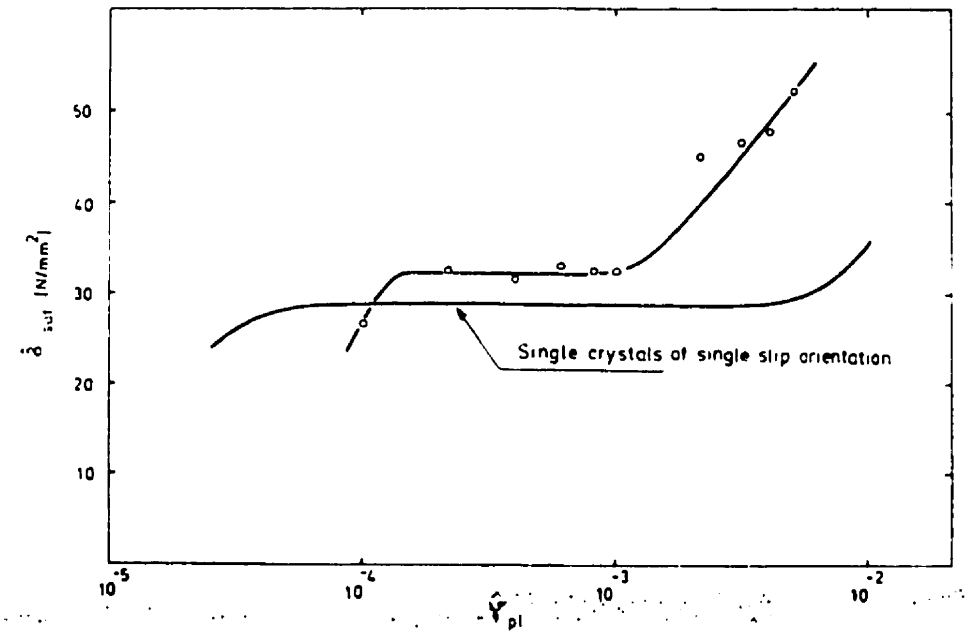

Figure 2.6 CSSC for 2mm-grained copper cycle under constant strain amplitude control, from Ref. [20]

Liu and Bassim [23, 32] reported a plateau-like behavior in their study on cyclic response of copper polycrystals. The material used was 99.4% pure copper with a grain size of 42μm. The test was conducted at room temperature under symmetric tension-compression fatigue at constant total strain amplitude control with an approximate constant plastic strain rate of 10^{-4}. Figure 2.7 shows the resulting C.S.S.C, where exhibits three regions of cyclic hardening. A plateau-like region, where the stresses show a slow constant increase, is observed in the plastic strain range of 1.5×10^{-5} to 7.5×10^{-4}.

Mughrabi and Wang [19] studied and discussed the cyclic behavior of polycrystalline copper under strain control over a range of plastic deformation amplitudes covering six orders of magnitude. The specimens used have a grain size of 15um, which is considered very small. The test was performed using incremental step method. They noted four different regimes where the fourth one is at very high amplitude of plastic deformation (Figure 2.8). It can be seen that the second region also shows a plateau-like behavior where the stresses increase slowly than those in the other regions.

2.2.1.3 Non-plateau behavior in C.S.S.C for copper polycrystals

A cyclic stress strain curve shown in Figure 2.9 was reported by Polak and Klesnil [26]. Their result was obtained by testing 30μm-grained specimens under strain amplitude control with a constant strain rate of 2×10^{-2}/s. They claimed two distinct regions in the curve and slope of the curve suddenly changes at plastic strain amplitude value of 7×10^{-4}.

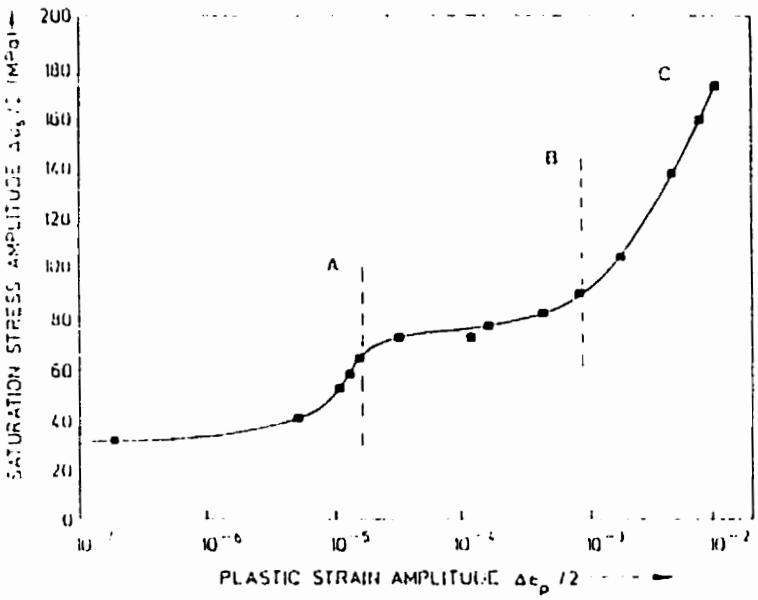

Figure 2.7 CSSC for 42μm-grained copper cycled under constant strain control with a constant low plastic strain rate, from Ref. [23]

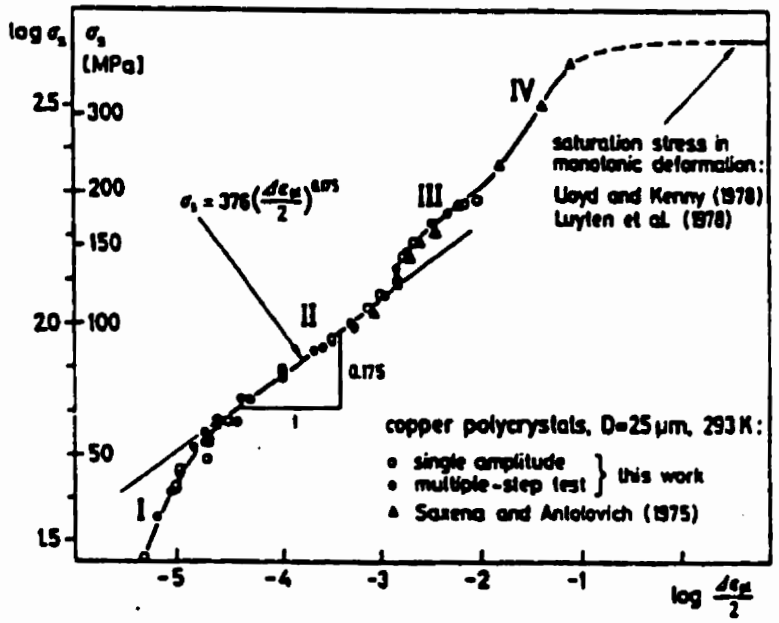

Figure 2.8 CSSC for 25μm-grained copper cycled over a wide range of plastic strain amplitudes, from Ref. [19]

Lukas and Kunz [28] found a non-plateau behavior in 1.2mm- and 70um-grained (Figure 2.10) copper ploycrystals, respectively. The test was performed under total strain amplitude control with a frequency of about 100Hz, which is considered very high.

2.2.2 Cyclic mode and strain rate effect on the cyclic behavior of polycrystalline copper

Only a few papers have been published on the effects of cycling mode on the C.S.S.C of copper polycrystals. In contrast to the tension test, fatigue can be conducted in many different ways, which may be one of the factors causing the scatter in the literature. The most common ways are: constant stress amplitude tests (load control), increasing stress amplitude tests (ramp-loading method), incremental-strain step control, decremental-strain step control and constant total or plastic strain amplitude tests (strain control).

Figueroa *et al.* [18] found that if polycrystalline copper was cycled under load control, there is a plateau behavior at stress values of 70Mpa approximately. On the other hand, if the tests were performed in strain control the plateau behavior was not observed, even though a change in slope occurred at a stress value of 64 Mpa.

History effects in the cyclic response of copper polycrystals, in terms of variable amplitude testing, were studied by Liu and Bassim [30]. The experimental result (Figure 2.11) shows the specimens tested at incremental strain amplitudes have the same stress as at conventional constant strain amplitude. However, the specimens tested

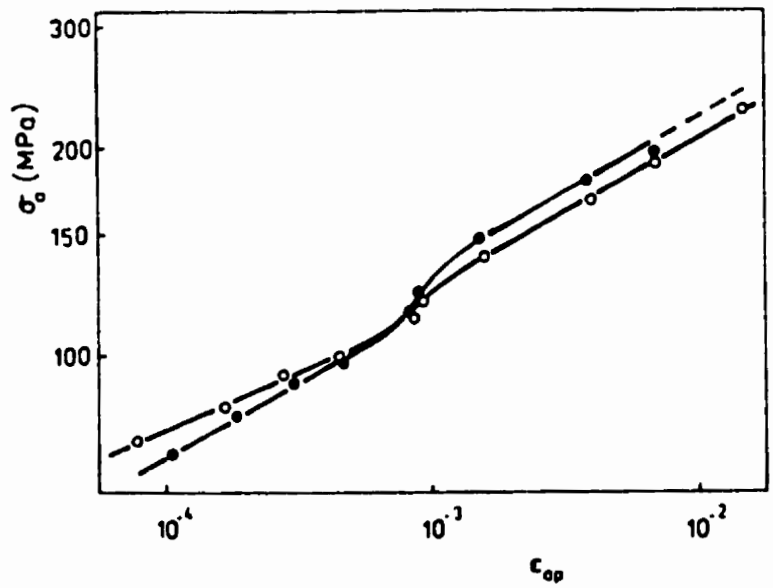

Figure 2.9 CSSC for 30μm-grained copper cycled under strain control with a constant high strain rate, from Ref. [26]

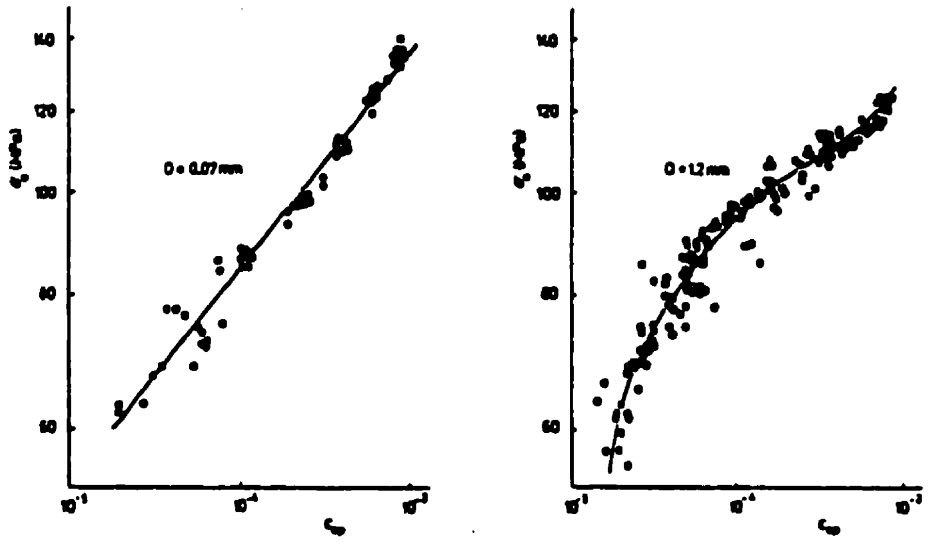

Figure2.10 CSSC for fine-grained and coarse-grained copper, from Ref. [28]

at decremental strain amplitude have a history effect on the saturation stress as compared with those at constant strain amplitudes control.

Neumann *et al.* [41] has suggested that the observation of strain instabilities occurring during cyclic hardening associated with localization of deformation, is related to the slow increase of the stress amplitude during his unique method of reaching saturation (ramp-loading method). Yan *et al.* have found that the cyclic deformation tends to be more strongly localized than in tests at constant amplitude if the tests are initiated by the ramp-loading method used by Neumann *et al.*.

Mayer and Laird [38] studied influence of cyclic frequency on strain localization and cyclic deformation in copper fatigue. In their study three frequencies were employed: 0.5, 2 and 8 Hz. They claimed that there is significant effect of the frequency on cyclic response, and, of course, the microstructures. They found that occurrence of persistent slip bands, which would affect cyclic response, is more pronounced at low cyclic frequency than at high frequency.

Yan *et al.* [42, 43] also investigated frequency effect on cyclic behavior. The test mode used was load control; and two different frequencies, 2 and 34 Hz, were used. They found that the copper cycled at 2Hz formed persistent slip bands (PSBs) quickly and showed a higher plastic strain than that cycled at 34Hz. These results suggest that PSBs nucleate more easily at lower loading frequencies.

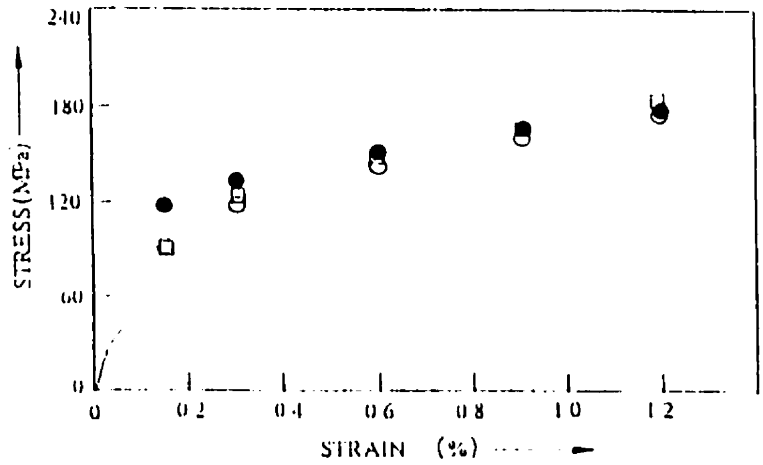

Figure 2.11 Saturated stresses of polycrystalline copper under various modes of control, from Ref. [30]

Furthermore, even using the same cyclic mode there are some dispute among the authors. In general, they relate to the use of different testing machines and experimental conditions.

2.2.3 Grain size effect on the cyclic behavior of polycrystalline copper

There are observations that indicate a role of grain size in the cyclic behavior of polycrystalline materials: 1) fatigue cracks have frequently been found to lie in or near grain boundaries [44]; 2) fatigue life is sometimes lengthened by a reduction in grain size [45].

Mughrabi *et al.* [46, 47] studied the influence of grain size on the fatigue behavior of copper polycrystals and found that a reduced grain size leads to an increased number of cycles to fracture, the effect being more pronounced at low strain amplitudes. They explained that intergranular fatigue crack initiation occurs commonly in the high-cycle fatigue range as a result of PSBs impinging on grain boundaries (GBs) and that PSB-GB cracking is more effective for larger grain size.

A survey of the literature shows that grain size effects in cyclic deformation are scarce and controversial. Mulliner *et al.* [27] studied the effect of grain size and test frequency on the fatigue behavior of copper polycrystals. The tests were run under constant total strain control with frequencies of 100Hz and 20Hz, on specimens with grain sizes of 25μm, 70μm, 350μm and 900μm (Figure 2.12). They concluded that finer grained

specimens have a fatigue limit of 58Mpa, which is larger than that for a coarser-grained material. There was no plateau in anyone of the C.S.S curves. However, it seems that grain size has an effect on slopes of the curves.

Pedersen [24] also observed a typical grain size effect in cyclic response for copper polycrystals (Figure 2.13). The test was performed under constant plastic strain control with a frequency of 1Hz, on the specimens with grain sizes of 85μm and 190μm. The results seem to reveal a small systematic increase of the saturation stress as the grain size decrease from 190μm to 85μm. He also indicated that this trend continues as the grain size is further reduced to 50μm. Higher saturation stress amplitude related to smaller grain sizes in cyclic deformation have been also reported in α brass [48] and nickel [49].

Lukas and Kunz [29] found that cyclic behavior of copper depended on grain size. However the result (Figure 2.14) shows an untypical grain size effect and no plateau behavior is observed for both grain sizes, which are 1.2mm and 70um respectively. The test was carried out under strain amplitude control; the frequency used was 100Hz.

Buchinger and Laird [50] basing their study on previous data, attempted to analyze the cyclic behavior of copper polycrystals in terms of true grain size but found that the reports of grain size were too unreliable to do so.

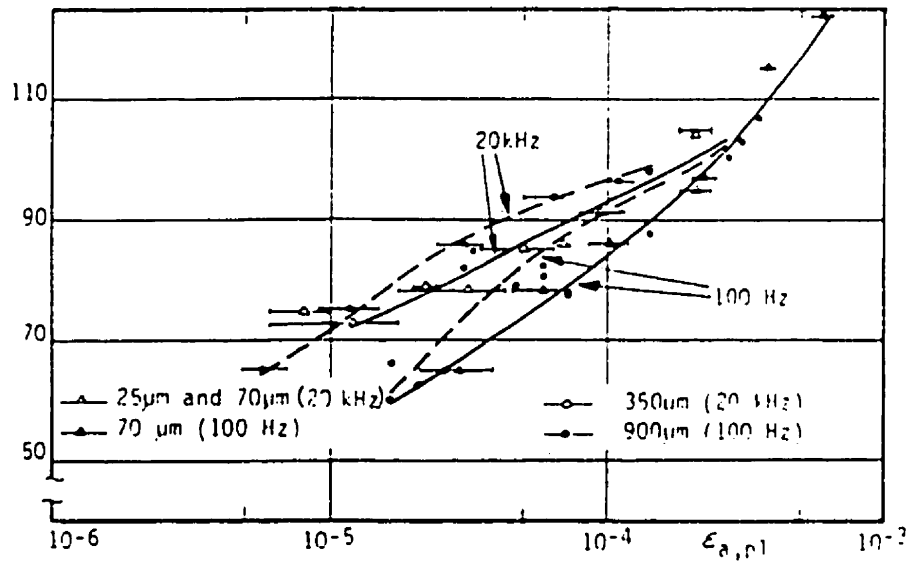

Figure 2.12 Grain size dependence of CSSC for polycrystalline copper tested various frequencies, from Ref. [27]

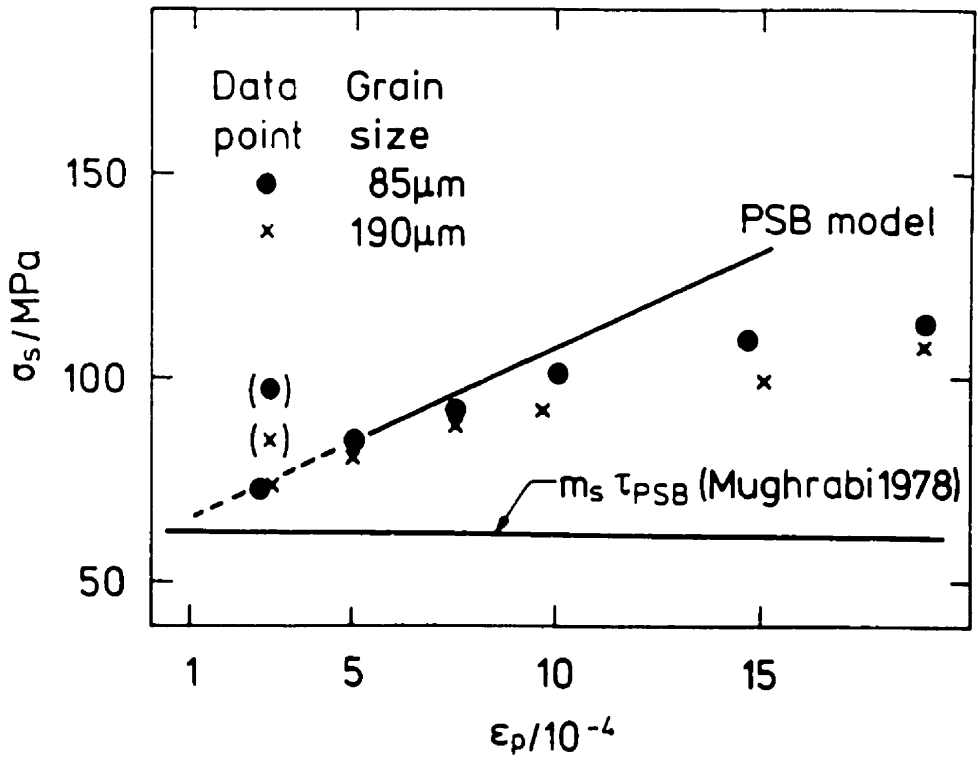

Figure 2.13 A typical grain size effect in CSS response for copper polycrystals, from Ref. [24]

2.2.4 Dislocation structures observation in copper polycrystals

Most of the above mentioned investigations focused not only on the determination of the cyclic stress-strain curve, but also on the analysis of associated microstructures, i.e., dislocation structures, persistent slip bands.

Figure 15 shows a schematic representation of the dislocation structures present at saturation in the low amplitude fatigue of copper as a function of testing mode. In general, in terms of stage to stage in the C.S.S.C, the dislocation structures of polycrystals are much more complicated than those for single crystals. The differences in dislocation structure between tests on stress and strain control were interpreted in terms of behavior at the onset of cycling. In stress control the high initial strains excite multiple slip, whereas in strain control, the slow build up of the stress enhances single slip behavior.

The dislocation structures of strain-control tested polycrystals with small grain size was studied by Liu and Bassim [23, 32, 64]. Based on their investigation, they found that the dislocation evolution could be characterized in terms of different regimes in the C.S.S.C obtained from tested 42.5um-grained specimens [Fig. 2.16a-d]:

Regime I: formation of loop patches (Fig. 2.16a) including cylindrical, irregular and cellular in shape.

Regime II: persistent slip bands (Fig. 2.16b) form from the loop patches in some grains.

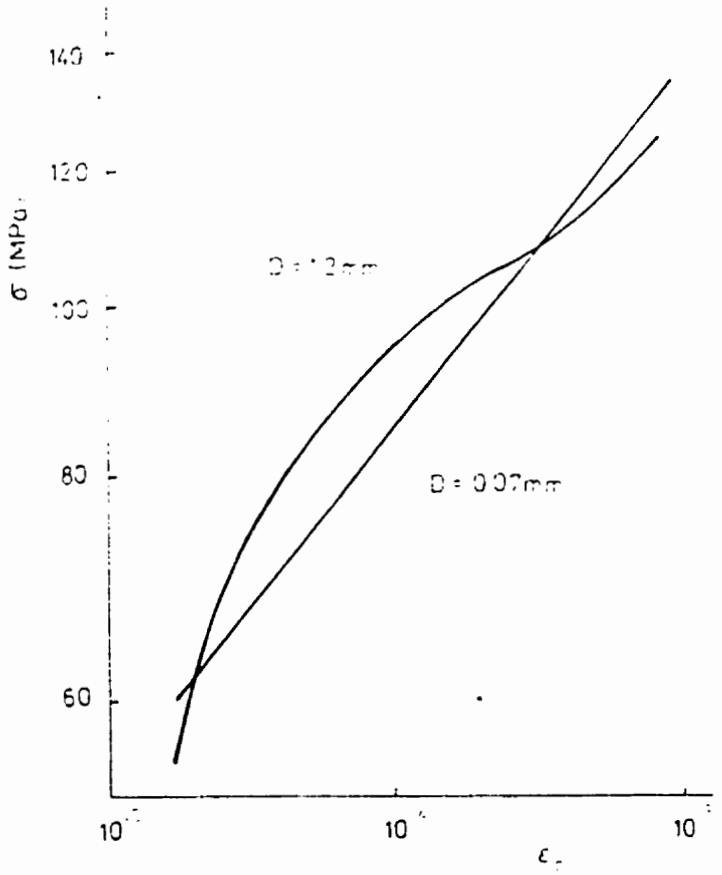

Figure 2.14 An untypical grain size effect in CSS response for copper polycrystals, from Ref. [29]

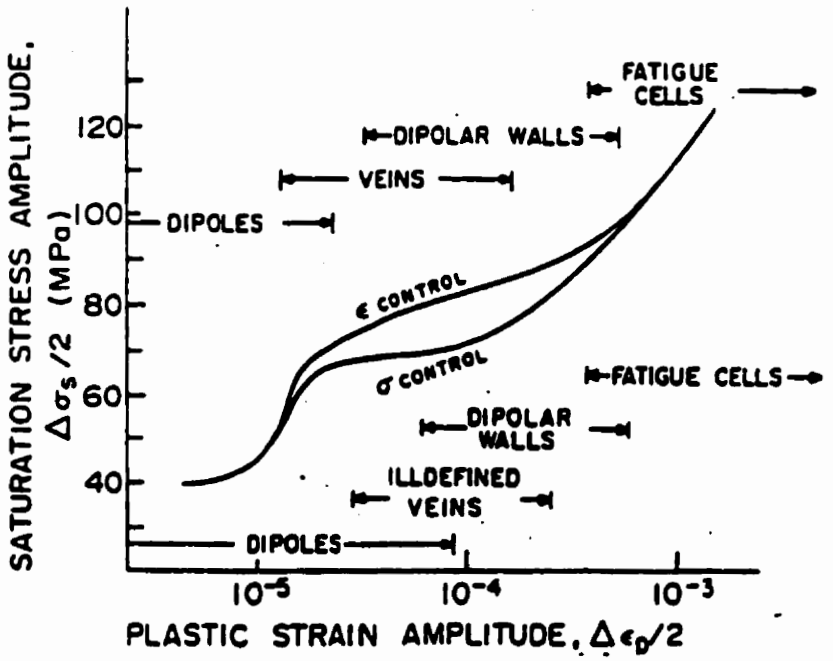

Figure 2.15 Schematic representation of the dislocation structures present at saturation in low amplitude fatigued copper, from Ref. [18]

Regime III: the dislocation structures are dominated by dipolar walls (Fig. 2.16c). In addition, labyrinth structures are also formed in this region. The dipolar walls become denser and sharper in image as the applied strain increases. At strain closes to the upper end, the dipolar walls become more cell shaped (Fig. 2.16d).

Moreover, Liu and Bassim compared dislocation structures in single crystal, coarse-grained polycrystals and small- grained polycrystals. They concluded that the evolution of dislocation structure under cyclic loading in coarse-grained (grain size >100um) copper, which is very similar to that in copper single crystal, is different from that in fine-grained polycrystals.

2.2.5 Persistent slip bands (PSBs)

Persistent slip bands generally form on polished surfaces of single crystal and polycrystals of ductile metals and alloys during low amplitude cyclic deformation. The early work of Thomson *et al.* [51,52] on polished surfaces of polycrystals and single crystals of copper showed that fatigue cracks start in PSB's and then gradually spread throughout the material. Lately, the understanding of the structure and behavior of PSB's has been greatly clarified by work on single crystals as reviewed by Brown [53] and Mughrabi [8]. The main implication of the single crystal work is that persistent slip is not confined to the metal surface. The ladder-like structure of PSB's takes place in the interior materials, which indicates that persistent slip is a bulk phenomenon in single crystals.

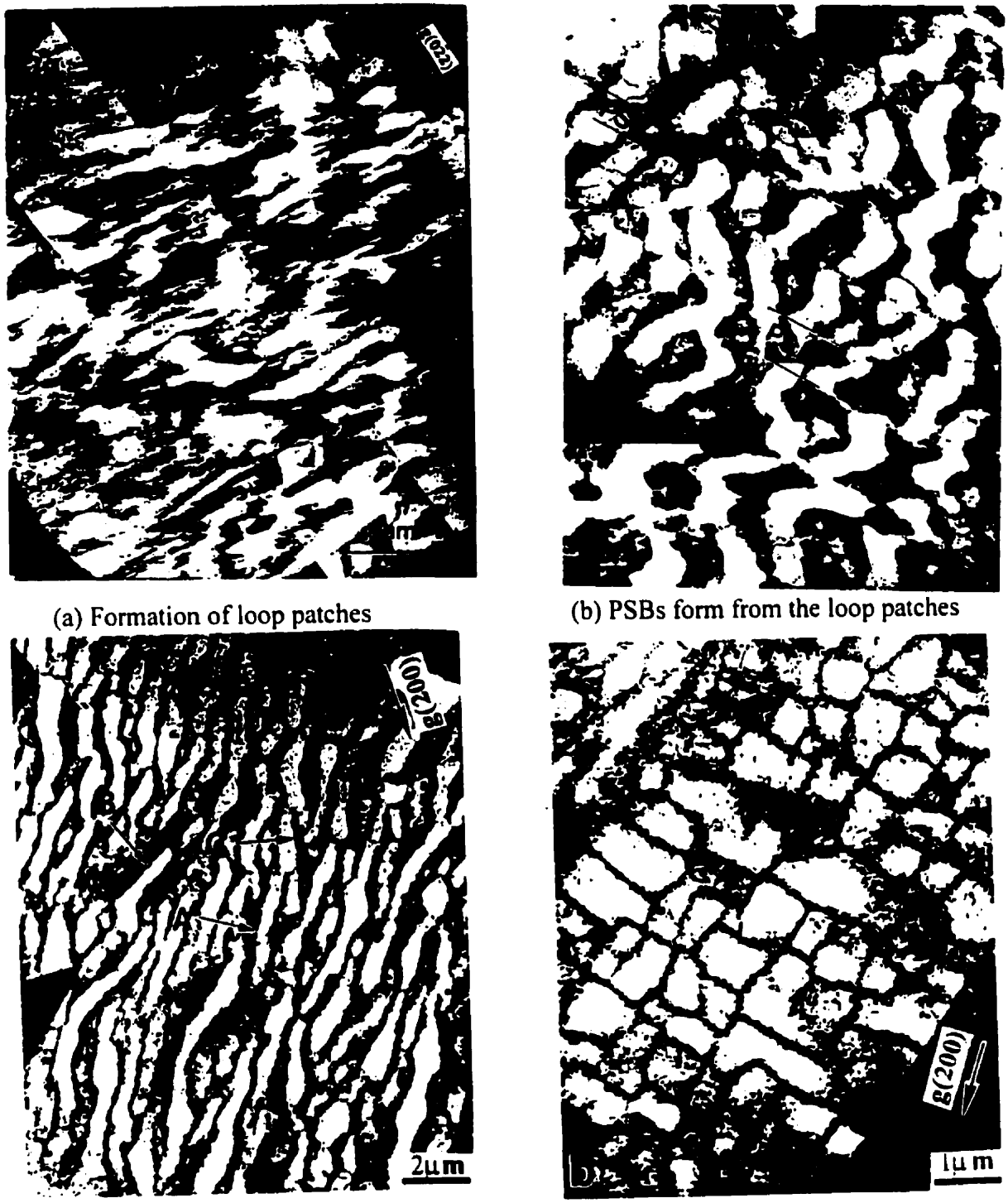

(a) Formation of loop patches

(b) PSBs form from the loop patches

(c) Dipolar wall structure

(d) Cell structure

Figure 2.16 Dislocation evolution in polycrystalline copper, from Ref. [64]

More recently, investigations on persistent slip bands in polycrystals have proved that it is also a bulk phenomenon in copper polycrystals (Figure 17a-b). Liu and Bassim [23,64] observed the initial occurrence of persistent slip band at the onset of the quasi-plateau in the C.S.S curve obtained from the study on 42μm-grained copper polycrystals and the amount of PSB's increases alone the quasi-plateau region. They also observed that even at the upper end of the quasi-plateau the volume friction of PSB's is less than 10%, which implies that the major contribution to the saturation stress is the bulk matrix around the PSB's. Therefore they concluded that the saturation stress in polycrystals is governed not only by the PSBs but also by the matrix in the quasi-plateau region.

The importance of study on occurrence of PSB's also lies on the prediction of fatigue life. It is established that the fatigue failure at low amplitude of stress or strain arises from the growth of microcracks nucleated in PSBs at the surface [54,55] and there is no mechanism for fracture if PSBs are absent. Therefore, the existence of threshold amplitude below which the PSBs do not form implies that the material exhibits a fatigue limit. In copper single crystal, the onset of the plateau indicates the occurrence of PSBs, so the corresponding strain or stress would be treated as fatigue limit. In copper polycrystals, where the presence of a plateau is still unclear, the fatigue limit would be determined by a stress or a strain below which PSBs do not occur.

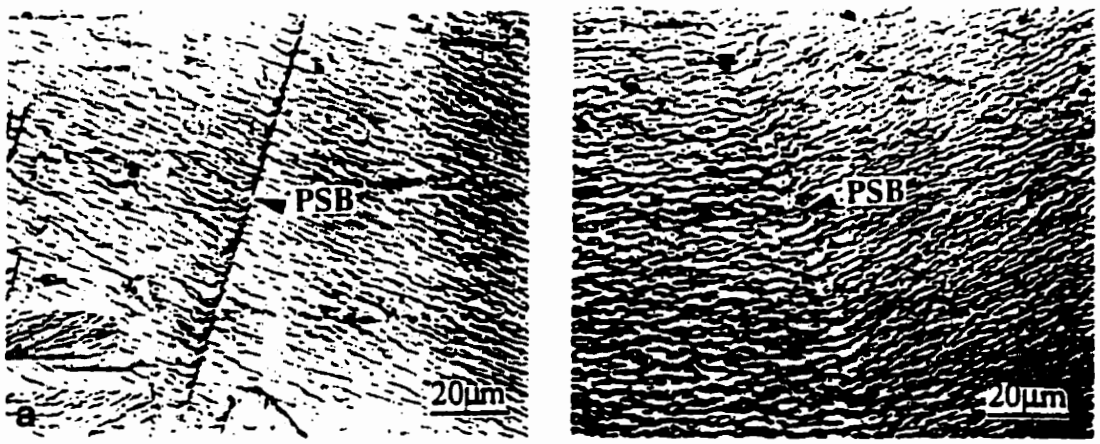

(a) PSB embedded in a vein structure (b) PSB formed at interface between two veins

Figure 2.17 The bulk behavior of PSBs in polycrystalline copper, from Ref. [23]

2.3 THE RELATIONSHIP BETWEEN THE CYCLIC STRESSES OF MONO- AND POLYCRYSTALS

In cyclic deformation, as in monotonic deformation, it is common to treat the deformation of polystals as the average behavior of agglomerate of individual crystallites and their interaction across the grain boundaries. Thus it is possible to relate the flow stress of the single crystal to that of the polycrystals by three models: Taylor, Sachs and the maximum Schmid factor. All of them can be formulated as:

$$\sigma = M \times \tau \qquad \text{and} \qquad \varepsilon = \gamma / M$$

Where σ = applied normal stress in the polycrystal.

ε = The axial plastic strain

τ = Resaved shear stress for the single crystal

γ = Resolved shear strain for the single crystal

M = Orientation factor, which is 3.06, 2.24, and 2 for the Taylor, Sachs and Schmid factor model respectively, for FCC materials.

In the Taylor model [56] the following assumptions are made: 1)-compatibility conditions are fulfilled, 2) the strains are the same in all grains and, 3) this uniform strain equals the macroscopic strain. In order to satisfy these conditions every grain has to undergo multiple-slip, generally on at least five independent slip systems [57]. Since this

model does not consider differences in stress states across a grain boundary, the equilibrium conditions are violated. The fact that compatibility conditions are fulfilled although the equilibrium conditions may be violated gives an upper bound for the yield stress of the polycrystals [58].

The Sachs model [59], on the other hand, assumes that the individual grains deform independently by single slip on their most highly stressed slip systems. The Sachs model, in combination with Eshelby's theory of internal stresses [60], has been popular for applying to cyclic deformation [17,25,61] because the plastic strain amplitude is small, compatibility can be accommodated elastically, and it is possible for only one slip system to be active in a grain.

In the maximum Schmid factor approach, it might be considered that plateau behavior will occur in the cyclic response of polycrystals because two investigations [18,19] found that the first PSB is formed at the stress given by the maximum Schmid factor, for tests under different cyclic conditions.

Kocks has pointed out [58] that there are compatibility problems about all these models and he concluded that there is no reason why one should ever use an average orientation factor, that is the mean of the Taylor and Sachs values. Some investigators have searched the possibility of combining elements from the two types of models. Kocks *et al.* [62] have proposed a modification to the Taylor model where maintenance of continuity across individual grains is the essential requirement, instead of simultaneous maintenance

of total continuity. On the other hand, Leffers [63], introduced a modified Sachs model where material continuity is fulfilled via the fulfillment of microscopic compatibility by secondary slip.

In contrast to Sachs and Taylor who do not consider the alternative possibilities of single and multiple slip, Kroner[65] concludes from continuum mechanics considerations that small plastic strains can be accomplished compatibly by single slip with some elastic accommodation, whereas higher strains provoke increasing internal residual stresses which enforce multiple slip. This suggests that, for the case of cyclic deformation, single slip will be possible in most grains with the exception of those orientated favorably with respect to the stress axis for multiple slip.

2.4 SUMMERY OF THE LITERATURE REVIEW AND THE RESEARCH OBJECTIVE

From the previous review, it can be concluded that the results on low cycle fatigue (LCF) of polycrystalline copper are different for different investigators. This might be attributed to the usage of various test conditions and grain sizes.

LCF study is one of the ongoing researches at the University of Manitoba. C. D. Liu, who was working with Dr. M. N. Bassim, had conducted a thorough investigation on the copper polycrystals with a grain size of 42um [23, 30-32, 64]. As a continuity of the

investigation, the test conditions used in the present study are identical to what C. D. Liu used.

The purpose of the present study is to investigate the grain size effect on the cyclic plastic stress-strain response of polycrystalline copper and to relate it to the observation of the persistent slip bands (PSBs).

CHAPTER 3: EXPERIMENTAL PROCEDURE

The copper rod stock was machined into cylindrical fatigue specimens. Different heat treatments were carried out on the specimens to get different grain sizes. Low cycle fatigue was conducted using a servo-hydraulic testing machine under constant strain amplitude control for a variety of strain amplitudes with a constant low strain rate. Cyclically saturated specimens were later sectioned for microscopic examination and analysis. This chapter provides the detailed description of the above procedures.

3.1 SPECIMEN PREPARATION

3.1.1 Obtaining Desired Microstructures

3.1.1.1 Metallographic Examination

In order to investigate the effect of grain size on the fatigue behavior, a series of grain sizes ranging from small to large were preferable. Therefore, preliminary heat treatments were conducted on the received copper to establish the effect of heat treatment temperature, time and pre-strains on the microstructure of the copper.

Samples for metallographic examination were sectioned from the as-received copper rod using a LECO CM-24A cutoff machine. The sectioned samples were subjected to various heat treatment schemes. The samples were then mounted in thermosetting bakelite resin

using a standard Buehler Simplimet II mounting press. Heating and cooling times of approximately 15minutes each and a pressure of 5 ksi ensured a good mount. Specimens were then polished mechanically using abrasive SiC papers on grinding wheels and a hand grinder table from 80 to 1200 grit followed by diamond polishing on polishing wheels typically up to 1μm diamond slurry and even LINDE B alumina abrasive when for high magnification observations and optical metallography. Although several etchants were tried it was found that an etchant consisted of 5g Fe $(NO3)_3$, 25ml HCL and 70ml water produced the best results.

3.1.1.2 Grain Size Measurement

Grain size measurement was conducted on the polished and etched samples using Leitz Analyzer, a programmable optical microscope. Although there are a variety of programs in the analyzer for automatic measurement, a manual counting program UMASTM.SIZ was employed because there was not enough contrast between grain boundaries and matrix in the copper for automatic counting programs.

Average grain sizes were measured using intercept counting with three line orientations; five parallel lines per screen, approximately 30 grains per image and over 20 images were analyzed for each heat treatment condition.

Table 3.1 presents the selected heat treatment schemes and resulting grain sizes.

Desired Grain Size (μm)	Annealing Temp. before Pre-strain (°C)	Pre-strain (%)	Annealing Temp. (°C)	Annealing Time (hour)
22	620	30	566	0.5
35	620	30	566	2.0
100			866	1.5

Table 3.1 Heat Treatments and Resulting Average Grain Sizes

3.1.2 Specimen Geometry

As described in Table 3.1, 30% plastic pre-strain was necessary to get 22μm- and 35μm-grained specimens. In order to avoid the effect of the specimen size on testing data, final specimen dimensions for testing were designed to be identical, which means that two different specimen geometries were designed for machining. Specimens that did not require pre-strain would be machined in accordance with ASTM specification E466 [66]. Specimens that needed pre-strained were machined according to the following adjustment

$$L = L' (1+x)$$

where L' = gauge length according to ASTM specification E466

L = gauge length for matching

x = percentage of pre-strain.

Assuming no change in volume during plastic deformation the adjusted diameter is obtained by:

$$r = r' (1+x)$$

where r = specimen diameter according to ASTM specification E466

r'= specimen diameter for machining

The required gauge diameter and gauge length were determined, according to ASTM specification E466, to be 6.5mm and 25mm, respectively. Figure3.1 and figure 3.2 show the geometrical dimensions of the specimen before and after plastic elongation.

3.1.3 Machining

The current low cycle fatigue testing was performed on three different grain sizes respectively, so the whole copper pieces were divided into three sets. One set was machined into the specimen geometry indicated in figure 3.1, while the other two sets of material were machined according to the specimen geometry shown in figure 3.2.

The quality of machining is critically important for the fatigue testing, so it is necessary to mention several main points for the proper method of machining:

Point 1. A piece of copper with a length of at least 18cm was cut from the received rod stock. Such a longer piece made it possible for a machinist to finish cutting threads on both sides in one time without detaching the piece from the lathe. In this way, specimen misalignment, which would cause buckling during a cyclic deformation, can be avoided.

Point 2. The piece was placed in the lathe and properly adjusted to make sure the whole piece would not be off center while rotating.

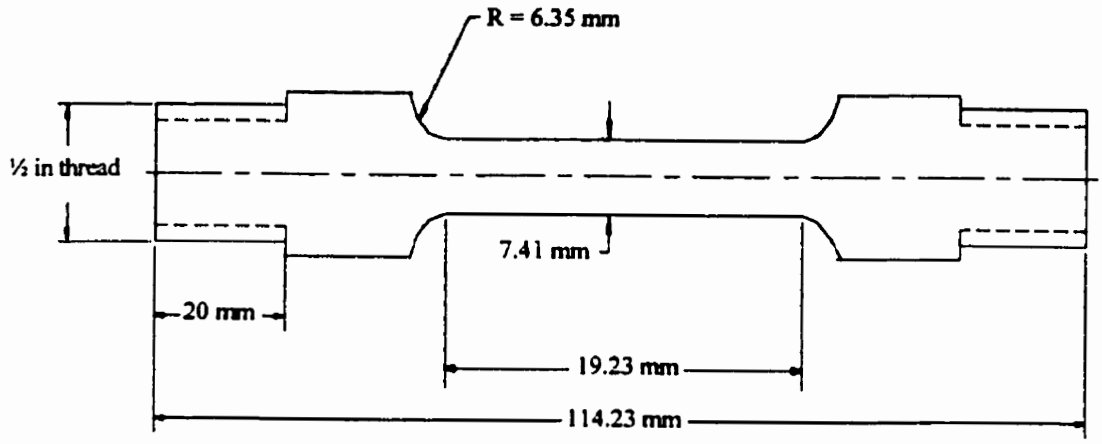

Figure 3.1 Dimension of specimen before pre-strain

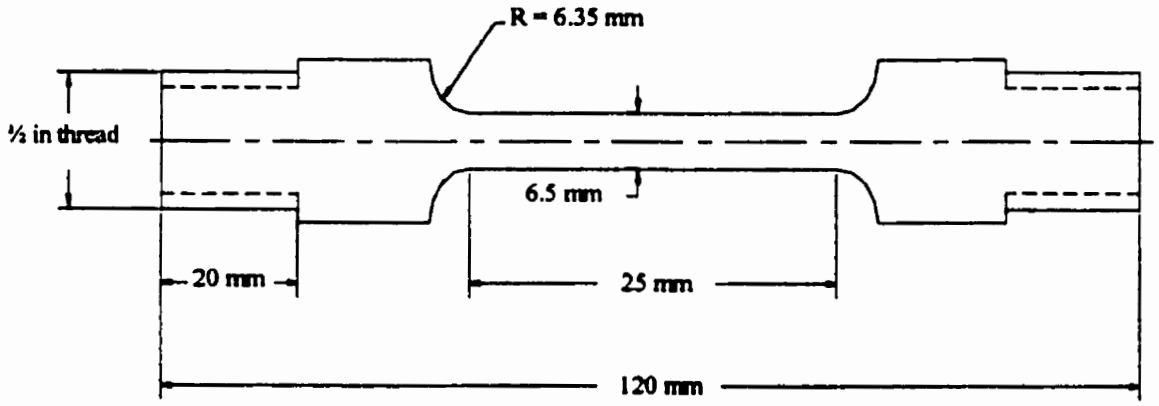

Figure 3.2 Dimension of specimen after pre-strain

Point 3. One end of the piece was centralized. Once this step was achieved, the piece was not removed from the lathe until the machining was completed. Otherwise, specimen misalignment would occur.

Point 4. Since copper is a soft material, threads on both sides of the piece should be cut first, before cutting the gauge section. Reversed procedures would lead to bending of the gauge section.

Point 5. Surface requirement was met by polishing, using fine grit paper #1200 and 6-microns diamond paste.

3.1.4 Heat treatment

As described in Table 3.1, three heat treatment schemes were performed to get three sets of specimens with a grain size of 22μm, 35μm and 100μm, respectively. A tube furnace (30° inclined) with argon protection atmosphere was used to perform the heat treatments to minimize surface oxidization. Pre-strain was conducted using a tensile testing machine.

The whole specimens were divided into 3 groups. One group of specimens, which would not be pre-strained, was heat treated at 866°C for 1 hour to get 100μm-grained specimens. The other two groups of specimens that would been pre-strained by 30% plastic elongation were first heat treated at 566°C for 2 hours and furnace-cooled to

eliminate internal stresses, so they could be allowed to be pre-strained by a relatively large plastic elongation. The plastic pre-strain was conducted on an INSTRON 1337 screw- driven Tensile Testing machine, which was connected with a personal computer, so testing date could be sampled and processed. Afterwards, one of the two groups was heat treated at 566°C for half an hour to get 22μm-grained specimens; the other group was heat treated at 566°C for 1.5hr to get 35μm-grained specimens.

3.2 LOW CYCLE FATIGUE TESTING (LCF)

3.2.1 Apparatus

The low cycle fatigue tests were conduced using an INSTRON 1332 servo-hydraulic testing machine, which was connected to an INSTRON 8500 programmable control unit. This machine has a load cell with a full load scale of 10000kg/10V and a variety of mounting fixtures to ensure that different shapes and sizes of specimens can be tested. All the testing parameters can be set up through the control unit: mode of testing can be determined by choosing stress, strain or position control. Values of frequency, displacement and waveforms can be written by means of the waveform control. etc.

An extensometer connected to the testing machine was used for the measurement of the strain amplitudes. This device has a maximum deflection of 1mm and an adjustable gauge length, which was 18mm for current usage. The extensometer was calibrated up to

0.2mm and set in the programmable control unit to increase the resolution of the strain-controlled testing.

A chart plotter was employed to record the data of the testing. The strain amplitude in displacement was plotted in the X-direction while the load amplitude was plotted in the Y-direction within a plotting area of 38cm by 25cm. A range of sensitivity from 0.25mv/cm to 5v/cm was adjusted corresponding to different signals from the testing.

3.2.2 Testing Procedure

The current testing was performed in symmetric tension-compression at room temperature. Each set of specimens with the same grain size was cyclically deformed for a variety of total strain amplitudes that range from approximately 5×10^{-6} to 5×10^{-3}. All specimens were cyclically saturated at a constant plastic strain rate of 10^{-4} until saturation occurred. Figure 3.3 shows the testing setup. The following steps show how the test was performed:

Step 1. Amplitude control was set in position mode, so the hydraulic actuator could be adjusted for loading a specimen. After position adjustment, the specimen was bolted into the mounting fixtures of the testing machine and locked into place by threading in a nut on each shoulder of the specimen. The bolts of the mounting fixture were slightly tightened by hand to avoid pre-load on the specimen.

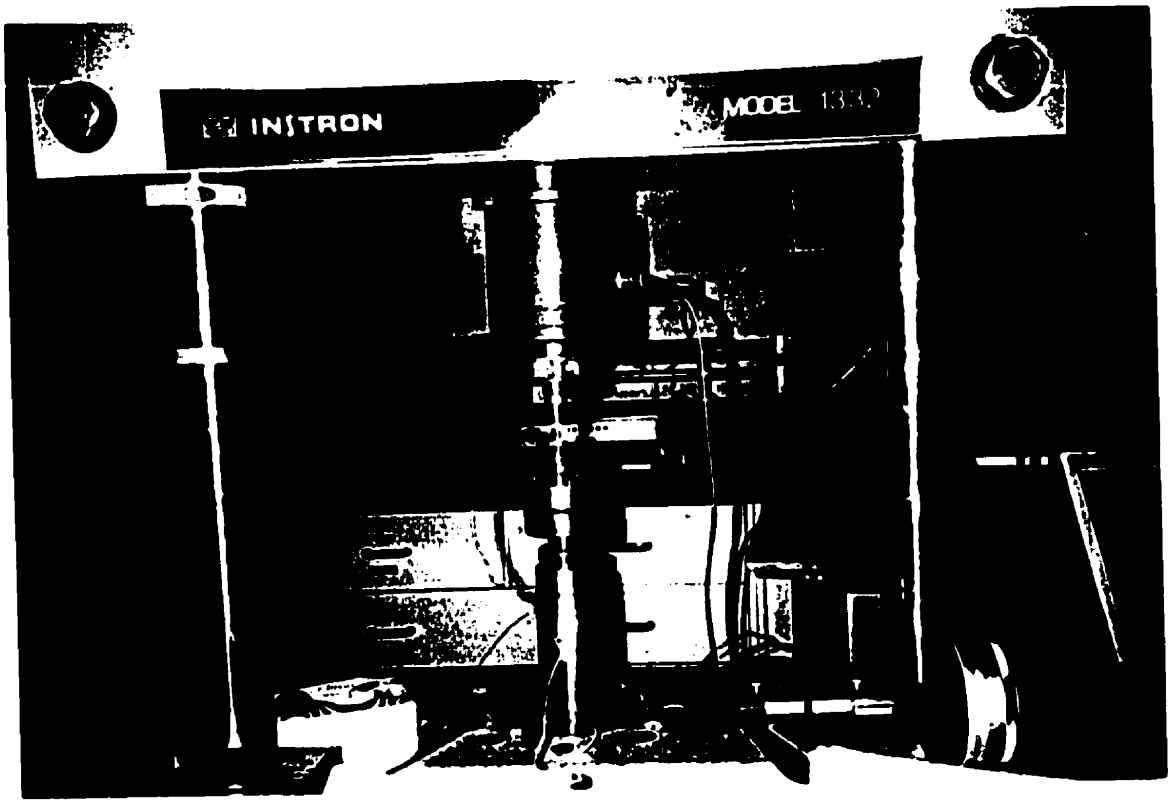

Figure 3.3 Testing setup

Step 2. Amplitude control was transferred from position mode to load mode. The load set point was set to zero, so that tightening could be performed without pre-load added on the specimen.

Step 3. The calibrated extensometer was attached to the gauge section of the specimen and balanced, so that the programmable control unit registered zero strain. After those, testing parameters including strain amplitude, frequency and triangular waveform were set through waveform channel on the INSTRON 8500 control unit. Finally, all limits for position, load and strain were set to ensure a safe and good testing.

Step 4. Amplitude control was transferred from load mode to strain mode from the control unit. Sensitivities were selected for both X- and Y- direction on the chart plotter, according the strain amplitude which would be applied.

3.3 POST-TEST SAMPLE PREPARATION AND EXAMINATION

In order to examine the persistent slip bands (PSBs) characteristics as well as other features, samples for optical microscopy and scanning electron microscopy were prepared using the following procedures:

Firstly, gauge sections were separated from the tested specimens by an abrasive cutter. During the cutting, special care was taken to avoid deforming the samples in order to preserve as much as possible the morphology that was created during the LCF testing.

Secondly, all sectioned specimens were cut longitudinally in the middle section of the specimens. A spark cutter was utilized for this step to minimize the surface deformation.

Thirdly, the obtained semi-circular specimens were mounted, ground and polished following the same procedures described as that in section 3.2. The final step for the sample preparation was electro-etching.. The etchant used was same as C.D.Liu's which consisted of 80ml H_3PO_4 and 120ml water. An electric potential of 2.2V was applied between a stainless steel cathode and the samples, for about 20 seconds. Subsequently the samples were removed from the electrolytic bath and rinsed.

The etched samples were investigated using a JEOL JXA-840 and a PHLILIPS XL30 ESEM TMP scanning electron microscopes. PSB morphology examination was conducted under the SEMs because of higher depth of focus and higher available magnification than under an optical microscope. Throughout the examination, photographs describing the occurrence of the PSBs were taken for typical specimens.

3.4 EXPERIMENTAL EVALUATION

This section explains (1) how various frequencies were used for different applied strain amplitudes, (2) procedures for evaluating the obtained hysterisis loops to get cyclic stress- strain curves, and (3) quantitative microscopy of persistent slip bands (PSBs).

3.4.1 Evaluation of the frequencies used

The current test was performed under constant strain control with a constant plastic strain rate of 10^{-4}. In order to get cyclic stress strain curves, a variety of strain amplitudes were used for each set of specimens. Each strain amplitude applied had a corresponding testing frequency to maintain strain rate approximately constant. The relationship is described as:

$$f = \Delta\varepsilon/\Delta\varepsilon$$

where f= frequency

$\Delta\varepsilon$ = plastic strain amplitude

$\Delta\varepsilon$ = plastic strain rate (10^{-4} in this study)

The strain amplitude was given as a percentage, which needed to be interpreted, because the testing machine could only accept displacement of cycling. The strain amplitude in displacement is related to the strain amplitude in percentage and the tested gauge length of the specimen by the following equation:

$$\Delta\varepsilon = \Delta\varepsilon^* \, L$$

where $\Delta\varepsilon^*$ = strain amplitude in displacement

$\Delta\varepsilon$ = Strain amplitude in percentage

L= tested gauge length of the specimen (18mm for this study)

3.6.2 Evaluation of the obtained hysteresis loops

Cyclic plastic strain is a measurable physical quantity that can be directly related to fatigue damage. If a metal is cycled to produce plastic deformation of equal amount in both tension and compression, the resulting cyclic stress-strain response will produce a loop similar to Figure 3.4, which is called hysteresis loop. The mechanical parameters associated with the hysteresis loop are indicated on the figure [66].

During the current testing, a strain amplitude, ε_a, was held constant and the dependent variable were measured. For complete reversed strain–control, the width of the loop was the total strain range $\Delta\varepsilon$, thus

$$\Delta\varepsilon = 2\Delta\varepsilon_a$$

Furthermore, the height of the loop depicts the total stress range, $\Delta\sigma$. This is related to the saturation stress amplitude, $\Delta\sigma_s/2$, by the following equation:

$$\Delta\sigma = 2\Delta\sigma_s$$

Also, from the figure it was possible to determine the elastic strain $\Delta\varepsilon_e$ and the plastic strain $\Delta\varepsilon_{pl}$. Therefore

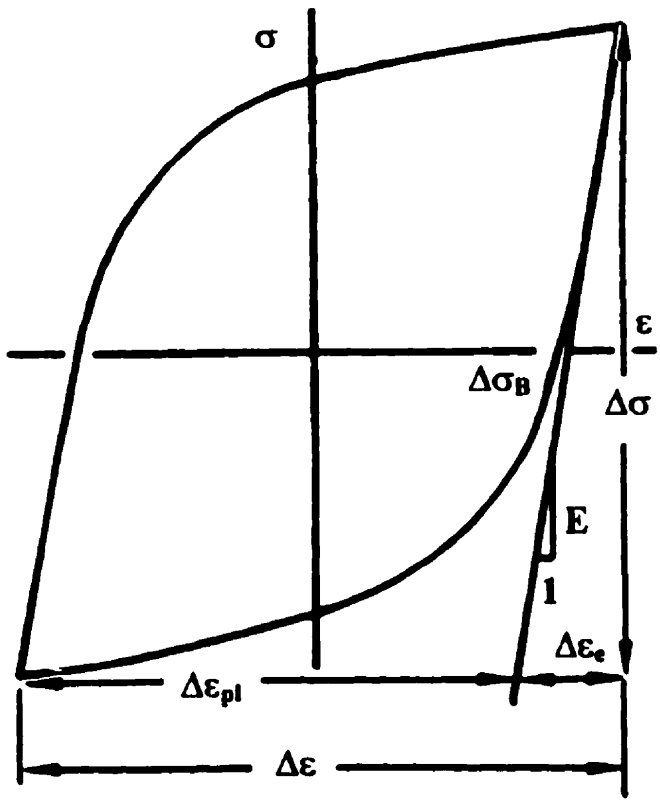

Figure 3.4 Schematic representation of steady-state stress-strain hysteresis loop

$$\Delta\varepsilon = \Delta\varepsilon_e + \Delta\varepsilon_{pl}$$

which after manipulation became

$$\Delta\varepsilon_{pl} = \Delta\varepsilon - \Delta\varepsilon_s$$

The specimens under a constant strain amplitude control eventually reached a steady stress, which was called saturation stress, $\Delta\sigma_s$; so the modules of elasticity, E, can be determined from the hysteresis loop obtained.

The plastic strain amplitude, $\Delta\varepsilon_{pl}/2$, is then related to the saturation stress amplitude, $\Delta\sigma_s/2$, and strain amplitude, $\Delta\varepsilon_a$, by the following equation

$$\frac{\Delta\varepsilon_{pl}}{2} = \Delta\varepsilon_a - \frac{\Delta\sigma_s}{2E} = \frac{\Delta\varepsilon}{2} - \frac{\Delta\sigma_s}{2E}$$

3.6.3 Quantitative microscopy of the PSBs

The cyclically saturated bulk materials were examined by the scanning electron microscopy. Widths of PSBs were measured from a photomicrograph by an equation [17]:

$$W = L/M$$

where L is the width measured from the photomicrograph and M is the magnification of the microphotograph.

In a similar way area fractions of PSBs were measured as [17]:

$$f = L_{PSB}/L$$

where L is the length of a straight line drawn perpendicular to the PSBs and L_{PSB} is the portion of the length covering PSBs.

CHAPTER 4 EXPERIMENTAL RESULTS

This chapter presents (1) material properties, which consists of material purity, pre-test microstructure and hardness. (2) The results obtained from the low cycle fatigue test, which includes hysteresis loops, the cyclic stress-strain curve for each grain size and observation of persistent slip bands. (3) Finally, all the C.S.S curves and corresponding microstructures were compared.

4.1 MATERIAL PROPERTIES

4.1.1 Material Purity

The chemical composition determination was conducted on a JEOL JXA-840, which is equipped with an Energy Dispersion Spectrometry (EDS) system.

According to the EDS examination, it could be seen that the current material is 99.94% purity copper. Other elements include aluminum and silicon, which only occupy 0.06% altogether. Table 4.1 and Figure 4.1 show the weight percentage of the EDS analysis and the quantification of the EDS spectrum, respectively. The copper peaks in Figure 4.1 are caused by the background matrix of copper.

Element	Percentage (weight)
COPPER	99.94
ALUMINUM	<0.01
SILICON	<0.005

Table 4.1 Chemical analysis of commercial copper

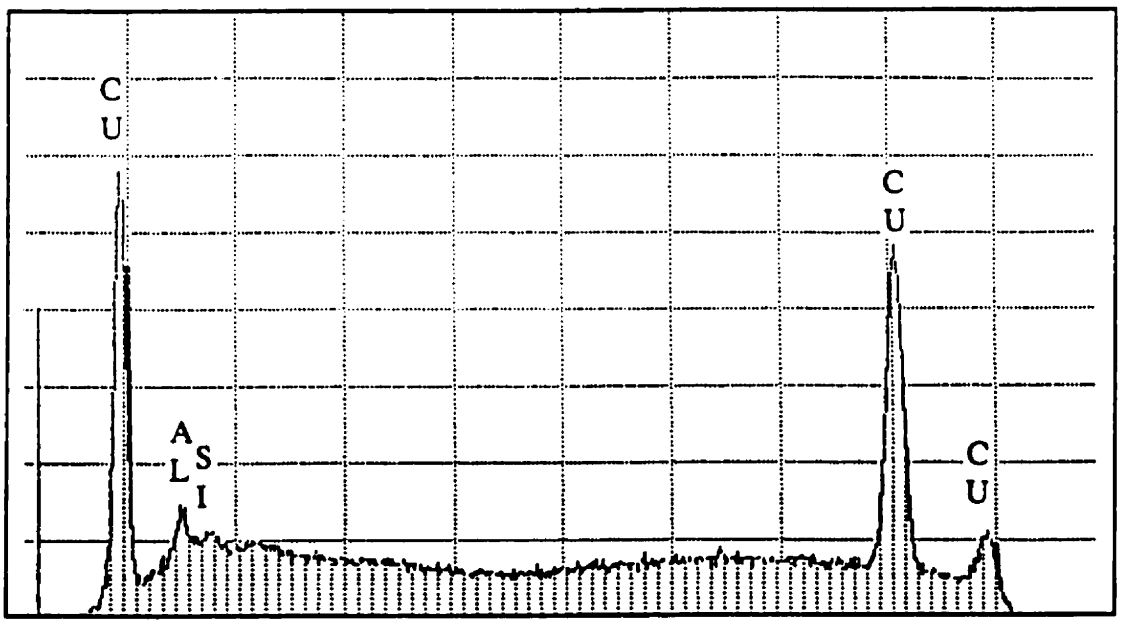

Figure 4.1 EDS analysis of the as-received material

4.1.2 Pre-test Microstructures

Optical examination of the copper on the etched samples revealed equiaxed grains as shown in Figure 4.2-4.4, which were taken for 22μm, 35μm and 100μm average grain size, respectively. All the pictures were taken at a magnification of 200× for ease of comparison.

Grain size distribution analysis was conducted and the results are provided in Table 4.2-4.4 for different annealing conditions. From the analysis, it can be found that the first annealing condition leads to a microstructure where grains ranging from 13μm to 26μm occupy 70% of the whole grains, while the second annealing condition causes a microstructure where almost 70% is occupied by grains ranging from 25μm to 60μm in size, and the third annealing condition leads to a polycrystals which has 90% of the grains occupied by 75μm to 140μm grains. Thus fine, medium and large-grained specimens were provided after the heat treatments being performed separately.

4.1.3 Rockwell Hardness

Although hardness testing was not critical to this study, it was interesting to establish the hardness of the material with different heat treatments; so, a Rockwell Hardness Tester was utilized at F scale.

Four hardness values were obtained for each sample with a certain grain size, and then

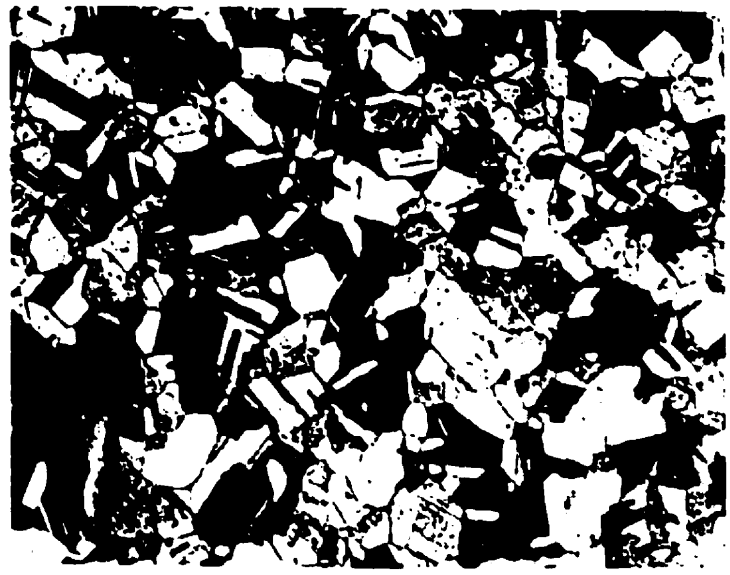

Figure 4.2 Polycrystalline copper with an averaged grain size of 22μm

Distributing G.S (μm)	10 - 12	13 - 17	18 - 22	23 - 26	28 - 32	33 - 37	38 - 42	45 - 50
Percentage (%)	12	20.6	26.8	19.8	6.1	4.9	4.9	4.9
Averaged G.S (μm)	22.7							

Table 4.2 Grain size distribution for 22μm average-grained material

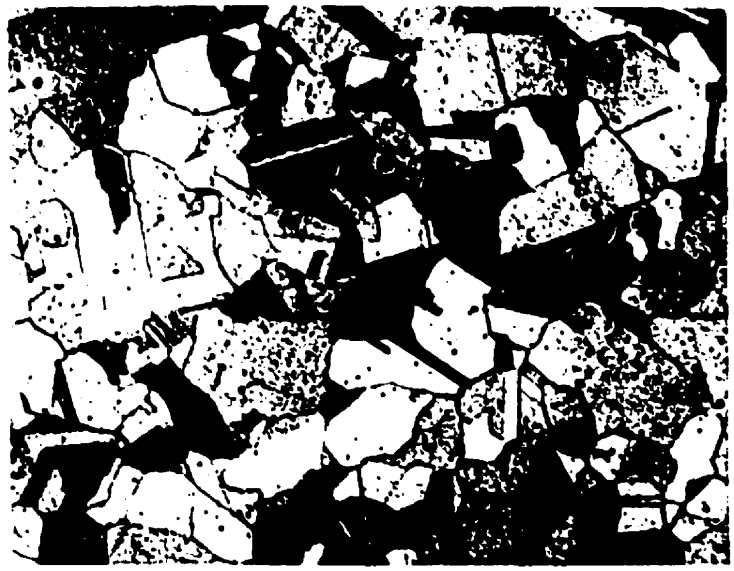

Figure 4.3 Polycrystalline copper with an averaged grain size of 35μm

Distributing G.S (μm)	12 - 16	20 - 27	28 - 36	37 - 45	47 - 60
Percentage (%)	13.8	28.9	20.3	21	16
Averaged G.S (μm)	34.5				

Table 4.3 Grain size distribution for 35μm average-grained material

Figure 4.4 Polycrystalline copper with an averaged grain size of 100μm

Distributing G.S (μm)	45 - 50	75 - 85	100 - 110	115 – 140
Percentage (%)	10	30	30	30
Averaged G.S (μm)	99.7			

Table 4.4 Grain size distribution for 100μm average-grained material

they were averaged to get a hardness value for that sample. The resulting measurement is present in Table 4.5, where the hardness values show a typical grain size effect, namely a highly hardness value for a smaller grain size.

4.2 HYTERISIS LOOP

From the test and corresponding cyclic stress-strain response, it was observed that all the specimens displayed only cyclic hardening until saturation occurred, which is consistent with earlier studies by others [18, 64]. The cyclic hardening observed in the present study is in contrast to reported testing results of copper single crystal [8], where pronounced softening before saturation was first observed [40] and where this softening increases with increasing resolved shear strain.

Figure 4.5 shows a typical stress-strain hysteresis loop for a specimen with 35um grain size tested under a constant strain amplitude of 3.6×10^{-3}. It was noticed that strain hardening was most pronounced in the early stage of cycling, and it was decreasing with increasing number of cycling until getting saturated.

The shape of hysteresis loops in saturation depended significantly on applied plastic strain amplitude. With increase of strain amplitude, the hysteresis loop was getting more rectangular than pointed in shape, which is in agreement with studies by Pedersen [24].

G.S (μm)	Averaged Hardness
22	53HBF
35	50HBF
100	47HBF

Table 4.5 Rock-well hardness for different grain sizes

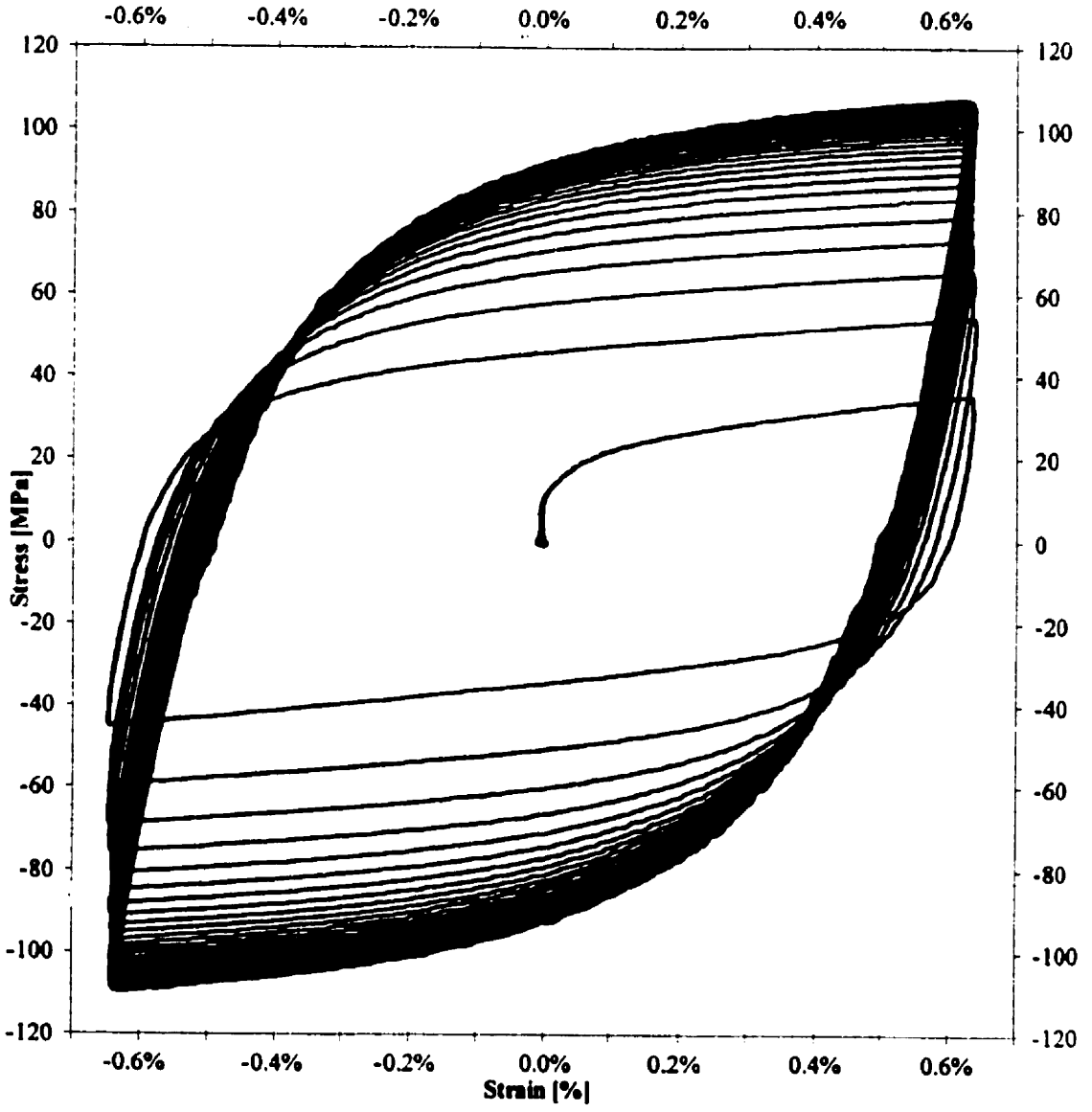

Figure 4.5 A Typical stress-strain hysteresis loop obtained for the present study

4.3CYCLIC STRESS –STRAIN CURVES AND CORRESPONDING MICROSTRUCTURES

The cyclic stress-strain curves were obtained by plotting all obtained saturation stresses amplitudes, $\Delta\sigma_s/2$, as a function of the plastic strain amplitudes, $\Delta\varepsilon_{pl}/2$. Following subsections present C.S.S curves and corresponding microstructural observation for each grain size.

4.3.1 C.S.S Curve for 22μm-grained material and PSB morphology

Low cycle fatigue on 22μm-grained copper polycrystals was performed on 13 specimens over a plastic strain range from 5×10^{-6} to 9.33×10^{-3} up to saturation. The test conditions were listed as shown in Table 4.6, where different frequencies were used for different strain amplitude to maintain a constant plastic strain rate.

4.3.1.1 The CSS Curve

Cyclic stress strain curve for 22μm-grained copper polycrystal were obtained by plotting the axial saturation stresses vs the corresponding axial plastic strain amplitudes as shown in Figure 4.6. The CSS curve reveals no obvious plateau, but it reveals clearly three regions of cyclic hardening. The first region, which is indicated as region A, appears at the plastic strain amplitudes below 3.2×10^{-5}; the second region (region B) extends from

Specimens	Frequency (Hz)	Total Strain	Plastic Strain	Saturation Stress (Mpa)
1	10	2.40E-4	5.00E-6	50
2	5	4.40E-4	2.10E-5	71
3	5	5.00E-4	3.20E-5	81
4	5	5.30E-4	6.67E-5	86
5	1.25	6.00E-4	1.10E-4	90
6	1.25	7.80E-4	1.50E-4	93
7	0.6	9.00E-4	1.80E-4	96
8	0.6	1.03E-3	2.36E-4	99
9	0.2	1.22E-3	3.75E-4	110
10	0.1	1.46E-3	7.00E-4	125
11	0.06	3.33E-3	2.10E-3	150
12	0.02	6.24E-3	5.10E-3	175
13	0.01	1.13E-2	9.33E-3	187

Table 4.6 Test conditions and cyclic response of 22μm-grained copper polycrystals cycled under constant strain control, with a low constant strain rate.

3.2×10^{-5} to 2.36×10^{-4} in plastic strain amplitude and the third region (region C) appears when the plastic strain amplitude is beyond 2.36×10^{-4}.

It can be found that in region A and region C, which correspond to low and high plastic strain respectively, the saturation stress increases markedly with increasing plastic strain amplitude. In region B, which corresponds to intermediate strain amplitude, the saturation stress increases less markedly with the increase of the plastic strain $\Delta\varepsilon_{pl}/2$ than that for the other two regions.

4.3.1.2 Microstructure Observation

Microstructure observation was conducted on the tested material to obtain a correlation between the mechanical properties and corresponding microstructure development. Figure 4.7 – 4.11 show the typical microstructure in fatigued 22μm-grained copper polycrystal for different regions.

The observation on the samples fatigued at very low $\Delta\varepsilon_{pl}/2$ shows no slip bands occurring throughout the whole region A. The occurrence of persistent slip bands started to be observed on a sample tested at a plastic strain amplitude of 3.2×10^{-5}, which is located at the lower end of region B. A typical PSB image is shown in Figure 4.7, it can be seen that a PSB occurred at this $\Delta\varepsilon_{pl}/2$ is not well-characterized as a ladder like structure and very few grains were observed to contain PSBs. However, nucleation of PSBs indicates the beginning of localization of deformation.

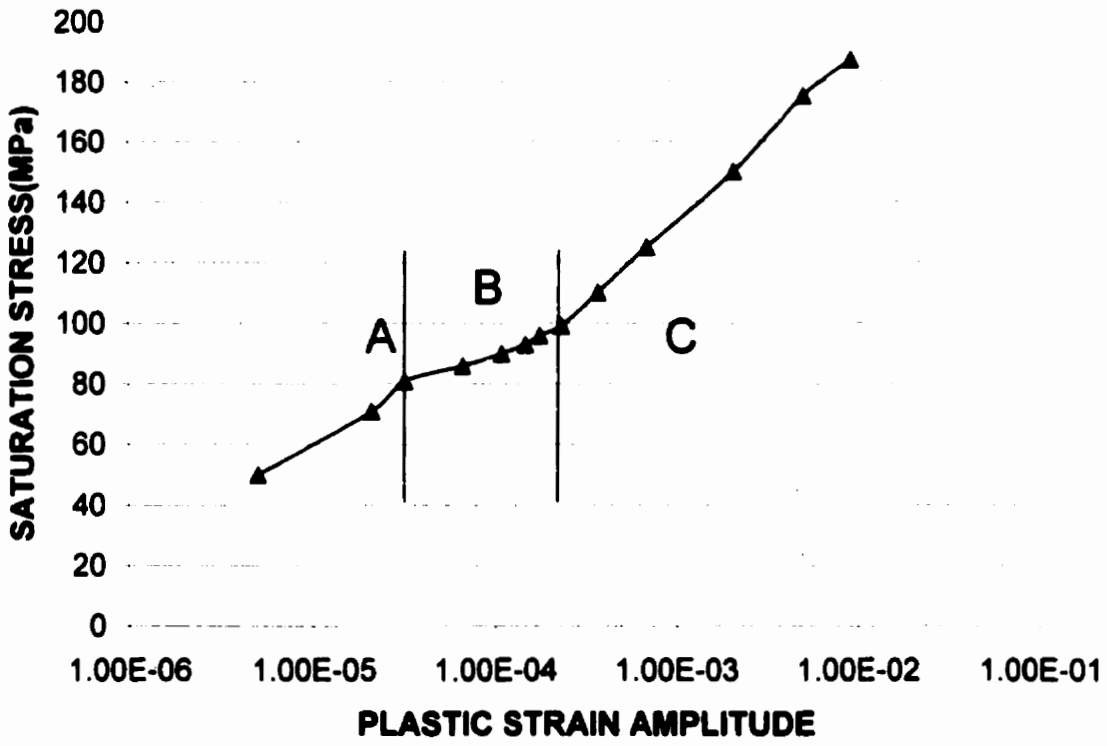

Figure 4.6 The CSS curve for 22μm-grained copper polycrystals

Figure 4.8 and 4.9 were taken for samples tested at $\Delta\varepsilon_{pl}/2$ of 1.1×10^{-4} and 1.8×10^{-4}, respectively, which are located within region B. Well-characterized PSBs, which show clear ladder-like rungs, were observed. It was noticed that a PSB starts form a grain boundary and extends toward the interior of the grain. Some of the PSBs just end up in the interior of the grain and most of them end up at the grain boundary of the other side.

Figure 4.10 shows an interesting morphology of PSBs: a pair of PSBs, which are parallel to each other. This picture was taken for a sample tested at $\Delta\varepsilon_{pl}/2$ of 2.36×10^{-4}, which is at the upper end of region B. According to the observation at this $\Delta\varepsilon_{pl}/2$, it was found more PSBs formed than that in the lower $\Delta\varepsilon_{pl}/2$. However there are only less than 8% of the grains containing PSBs.

Figure 4.11 is a microphotograph for a sample tested at $\Delta\varepsilon_{pl}/2$ of 2.1×10^{-3}, which is in the middle of region C. The image shows the occurrence of secondary slip bands. Based on the investigation over the samples in the region C, it was found that there was no clear increase of PSBs in amount. However, the occurrence of second slip bands was pronounced, which led to more rapid increase in saturation stress than that in region B.

Figure 4.7 Nucleation of PSB in 22μm-grained sample tested at a plastic strain of 3.2×10^{-5}

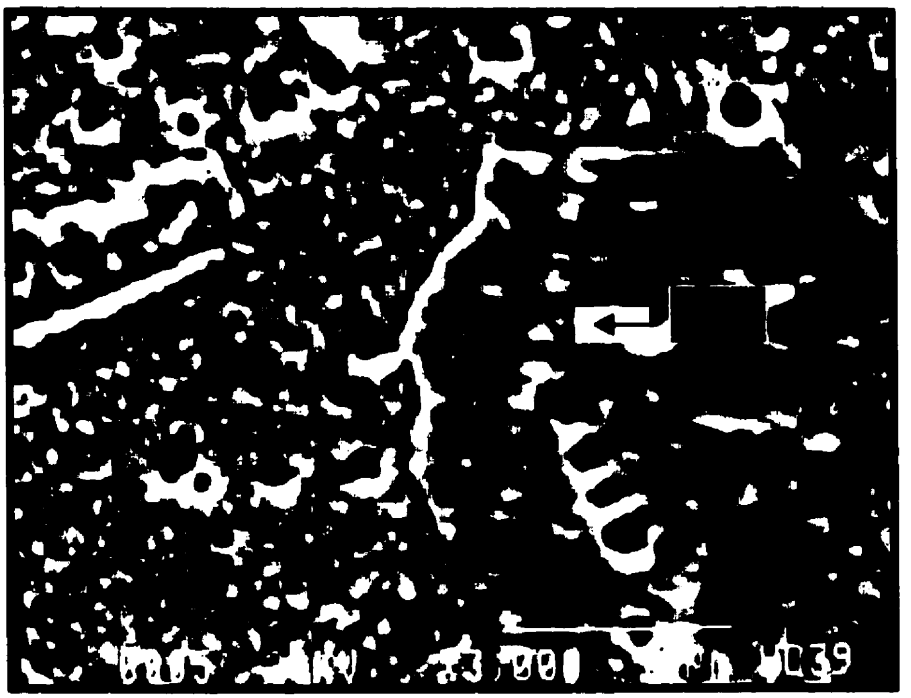

Figure 4. Well-characterized PSB in 22μm-grained sample testted at a plastic strain of 1.1×10^{-4}

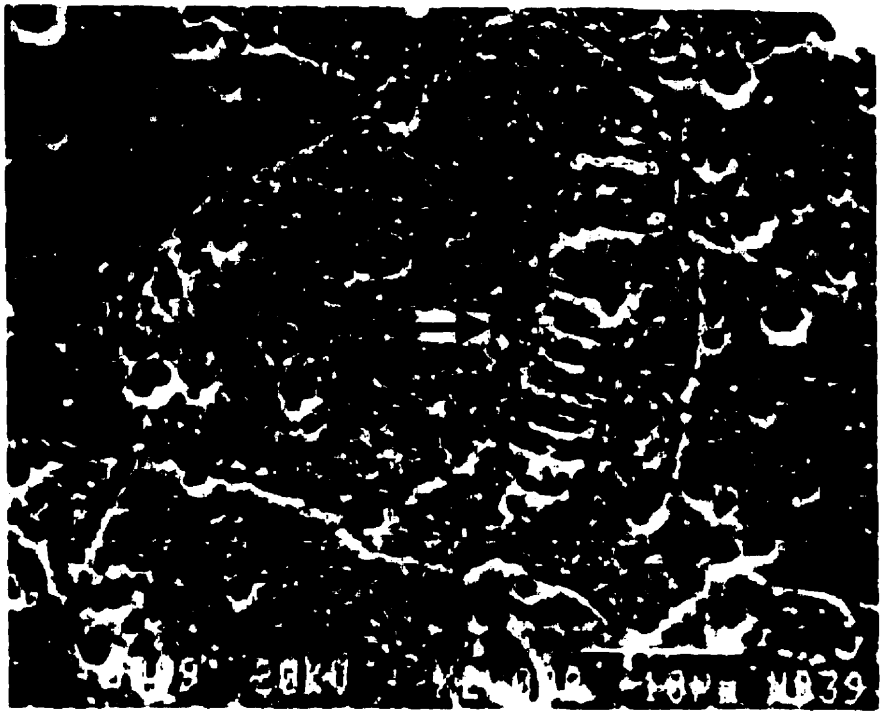

Figure 4.9 Ladder like PSB structure in 22μm-grained sample tested at a plastic strain of 1.8×10^{-4}

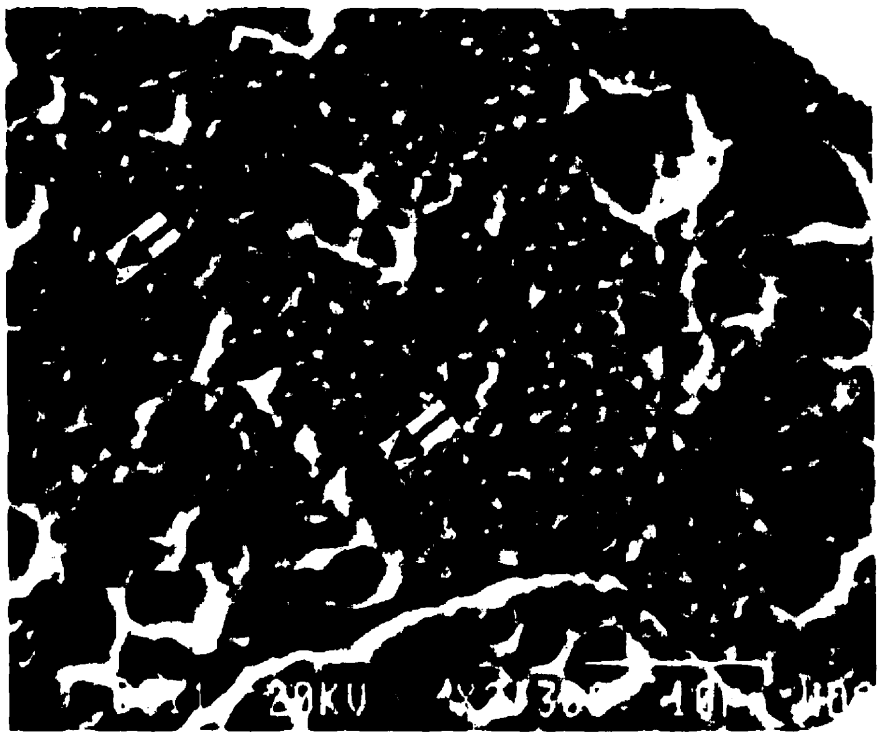

Figure 4.10 A pair of parallel PSB structure in 22μm-grained sample tested at a plastic strain of 2.36×10^{-4}

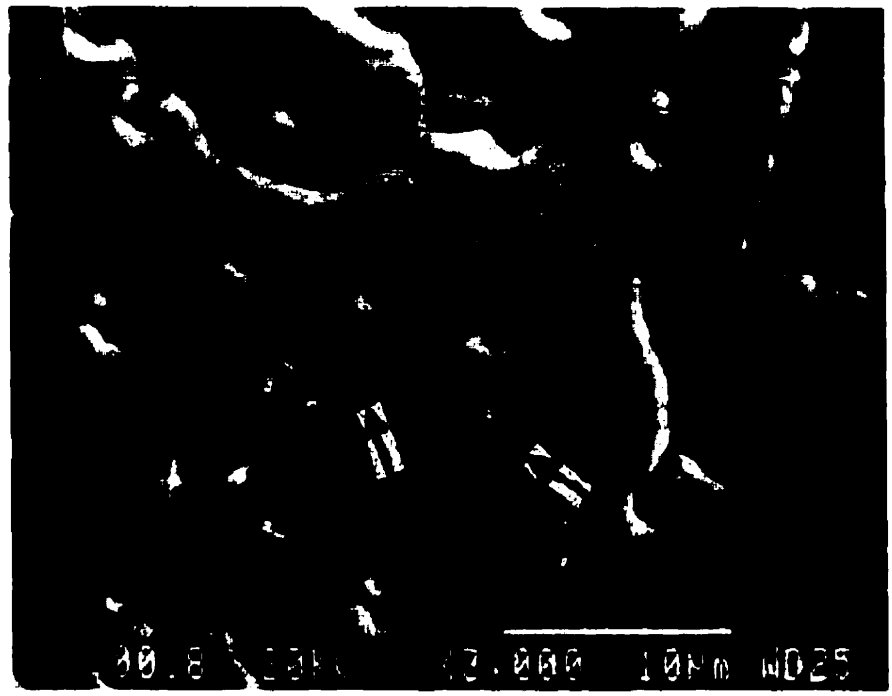

Figure 4.11 Secondary slip bands (SSBs) in 22μm-grained sample tested at a plastic strain of 2.1×10^{-3}

4.3.2 C.S.S Curve for 35um-grained material and PSB morphology

Similarly to the test for the 22μm-grained copper, 12 specimens with a grain size of 35um were cyclically deformed under constant total strain amplitude control with a low plastic strain rate of 10^{-4},over a plastic strain range from 5.1×10^{-6} to 8×10^{-3}. The test conditions are list in Table 4.7, where the values of the $\Delta\varepsilon_{pl}/2$ and $\Delta\sigma_s/2$ were evaluated from the obtained steady hysteresis loops.

4.3.2.1 The CSS Curve

The cyclic stress strain curve for 35μm-grained samples were obtained by plotting the $\Delta\varepsilon_{pl}/2$ values as a function of the $\Delta\sigma_s/2$ values in a semi-log paper as shown in Figure 4.12. It can be seen that the CSS curve shows distinct three regions of cyclic hardening. A quasi-plateau, where the saturation stress, $\Delta\sigma_s/2$, increases slowly with increasing plastic strain amplitude, $\Delta\varepsilon_{pl}/2$, extends from 2.6×10^{-5} to 6.8×10^{-4}. While in region A and region C, which correspond low $\Delta\varepsilon_{pl}/2$ and high $\Delta\varepsilon_{pl}/2$ amplitude, the saturation stress increases significantly with increasing plastic strain amplitude.

4.3.2.2 Microstructure Observation

In order to explore the connection between the obtained cyclic stress-strain response with corresponding microstructures, a SEM was used for searching the evidence. Figure 4.13 –

4.18 provide several typical PSB morphology in the tested 35μm-grained copper polycrystals at different $\Delta\varepsilon_{pl}/2$ amplitudes.

The images shown in Figure 4.13 and 4.14 were taken for a sample tested at $\Delta\varepsilon_{pl}/2$ amplitude of 2.6×10^{-5} and 2×10^{-5}, respectively, which is situated at lower end of the quasi-plateau. It can be seen from Figure 4.13: a pair of parallel PSBs is emerging from the surrounding matrix; the PSBs were initiated at the grain boundary and extending toward the interior of the grain. According to the investigation at this $\Delta\varepsilon_{pl}/2$ amplitude, it can be asserted that very few grains contained PSBs. The occurrence of PSBs just started at this point.

Figure 4.15 and 4.16 were taken for samples tested at plastic strain amplitudes of 5×10^{-5} and 7×10^{-5}, respectively, which are located within region B. The PSBs show clear ladder-like structure which started at one side of a grain boundary and ended at the other side of the boundary. Based on the investigation on the two samples, it can be said that the PSB population increases with the increasing $\Delta\varepsilon_{pl}/2$ amplitude.

Figure 4.17 was taken for a sample tested at $\Delta\varepsilon_{pl}/2$ of 6.8×10^{-4}, which is the end of region B. It can be seen that PSBs in two adjacent grains intersect each other at the grain boundary, but they run alone in different direction. This phenomenon was also observed and described by previous investigators [23,24]. According to the observation at this plastic strain amplitude, it was found that the amount of PSBs was more than that in the sample described in Figure 4.16. However, there is only less than 12% of the grains

Specimens	Frequency (Hz)	Total Strain Amplitude	Plastic Strain Amplitude	Saturation Stress (Mpa)
1	10	2.40E-4	5.10E-6	46
2	10	3.30E-4	1.00E-5	51
3	5	4.20E-4	2.00E-5	69
4	2.5	4.60E-4	2.60E-5	74
5	2.5	5.20E-4	5.00E-5	80
6	1.25	5.50E-4	7.00E-5	82
7	0.5	1.00E-3	3.60E-4	91
8	0.2	1.43E-3	6.80E-4	96
9	0.2	1.84E-3	9.50E-4	106
10	0.1	2.70E-3	1.64E-3	120
11	0.05	4.20E-3	3.00E-3	135
12	0.02	9.90E-3	8.00E-3	171

Table 4.7 Test conditions and cyclic response of 35μm-grained copper polycrystals cycled under constant strain control, with a low constant strain rate.

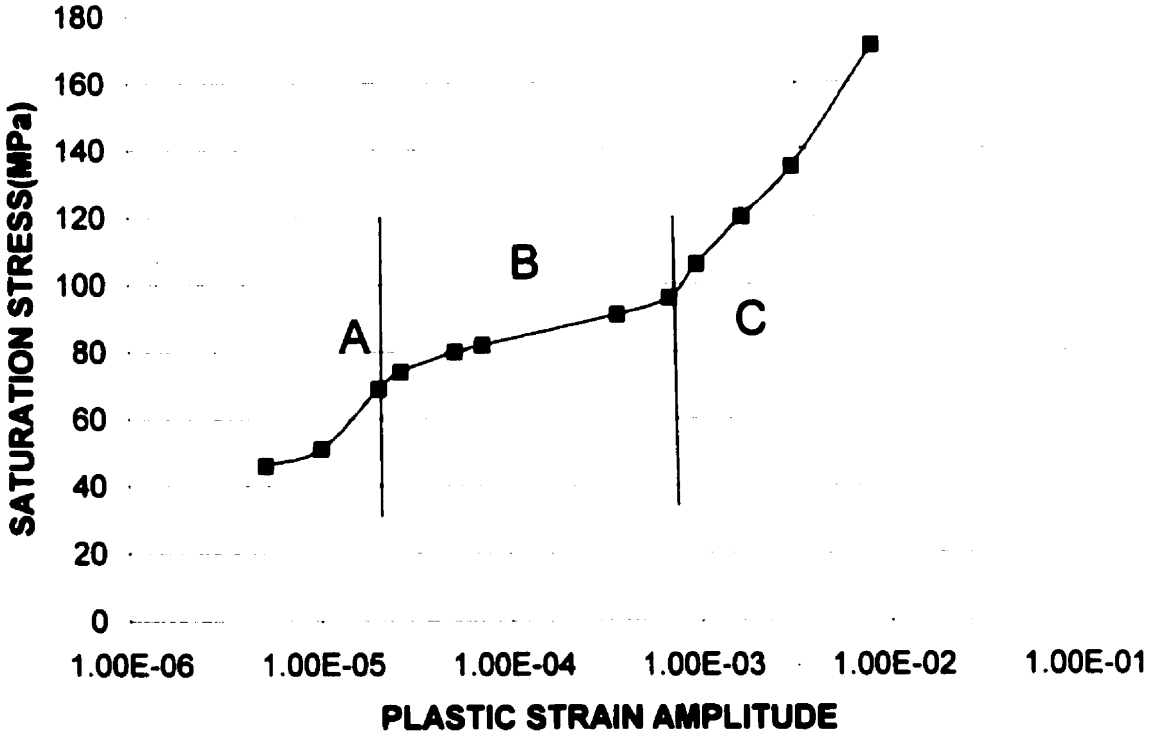

Figure 4.12 The CSS curve for 35μm-grained copper polycrystals

containing PSBs.

SEM observation on the samples tested at high plastic strain amplitudes, which are in region C, shows that there is no significant increase in PSB population. Formation of secondary slip bands was observed as shown in Figure 4.18, which corresponds to a sample tested at a plastic strain amplitude of 1.64×10^{-3}. The image shows a pair of parallel secondary slip bands. Normally, it is impossible to determine a PSB by distinguishing on which slip plane it occurred for scanning electron microscopy, however the unique character of ladder-like structure can be an indication of PSBs.

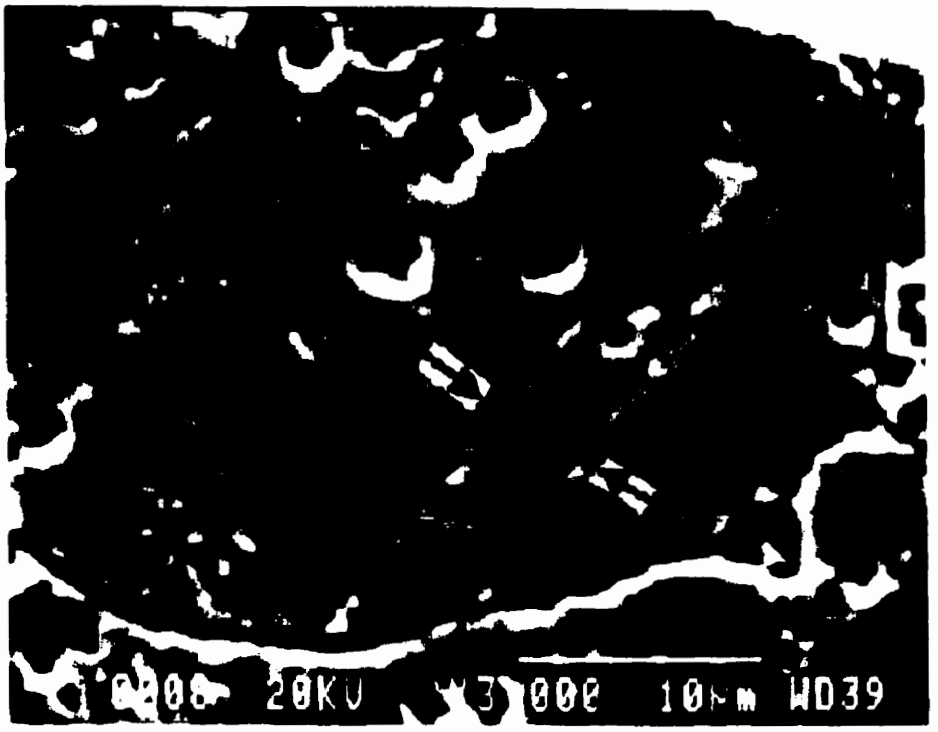

Figure 4.13 The emergence of a pair of parallel PSBs in 35μm-grained sample tested at a plastic strain of 2×10^{-5}

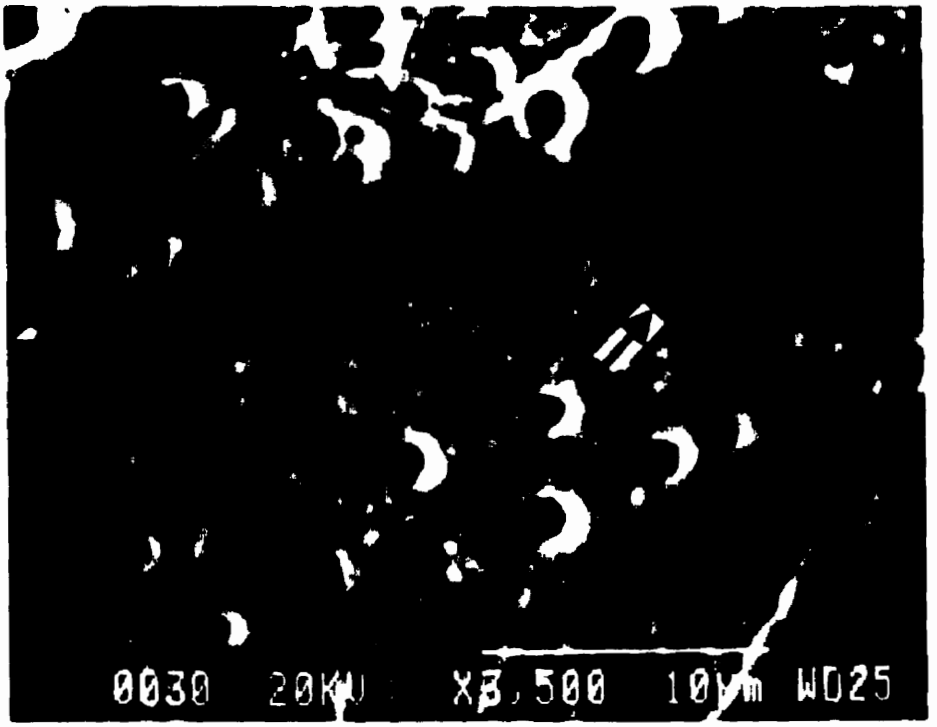

Figure 4.14 Ladder like PSB structure in 35μm-grained sample tested at a plastic strain of 2.6×10^{-5}

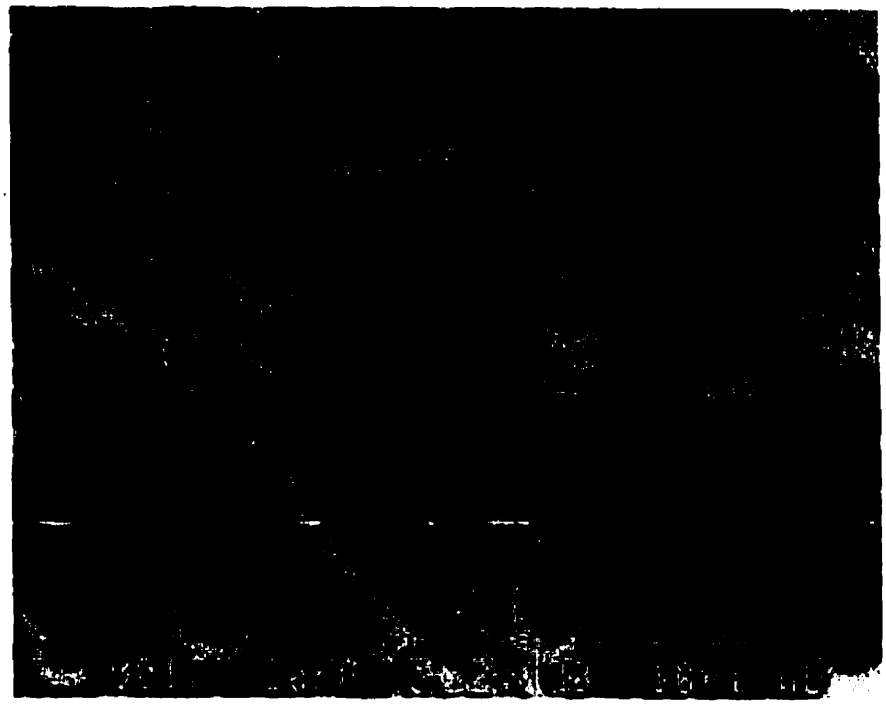

Figure 4.15 Ladder like PSB structure in 35μm-grained sample tested at a plastic strain of 5×10^{-5}

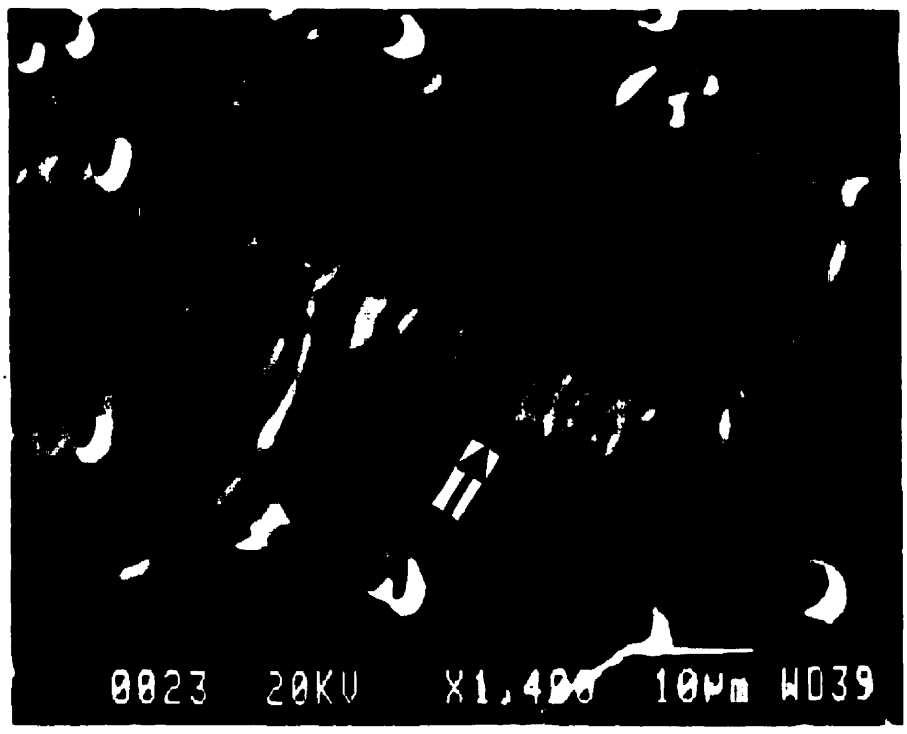

Figure 4.16 Well-characterized PSBs in 35μm-grained sample tested at a plastic strain of 7×10^{-5}

Figure 4.17 Intersection of PSBs in two adjacent grains in 35μm-grained sample tested at a plastic strain of 6.8×10^{-4}

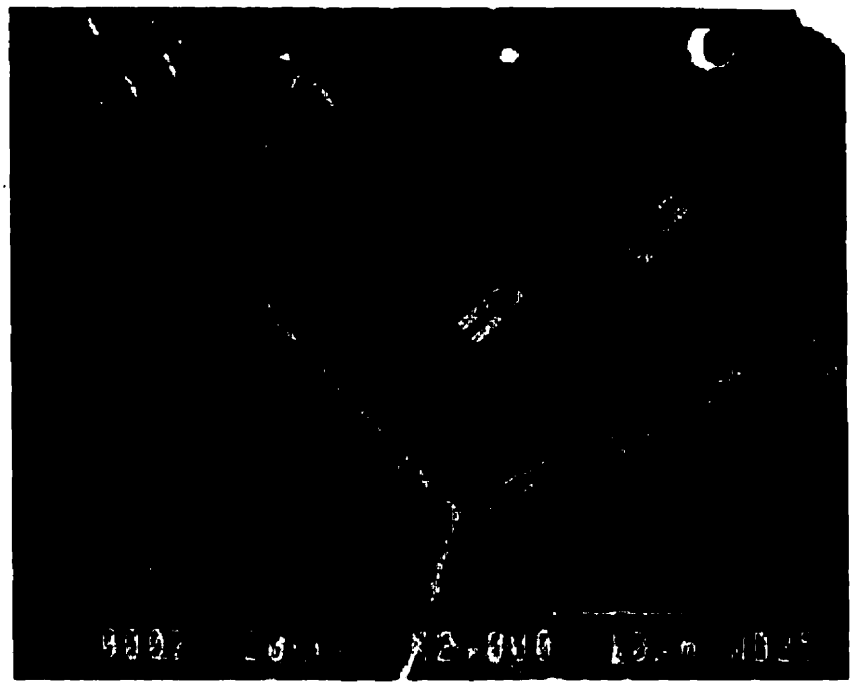

Figure 4.18 A pair of parallel secondary slip bands in 35μm-grained sample tested at a plastic strain of 1.64×10^{-3}

4.3.3 C.S.S Curve and the corresponding microstructure for 100μm grained material

Table 4.8 lists the LCF testing conditions and cyclic response for those specimens with an average grain size of 100μm. 12 specimens were tested for a variety of plastic strain amplitudes ranging from 5.3×10^{-6} to 5.22×10^{-3}. The test mode and plastic rate used for this grain size is the same as those for 22μm- and 35μm-grained copper polycrystals.

4.3.3.1 The CSS Curve

Figure 4.19 shows the CSS curve for 100μm-grained copper, which was obtained by plotting $\Delta\varepsilon_{pl}/2$ values as a function of the obtained $\Delta\sigma_s/2$ values. It is observed that the obtained CSS curve shows very clearly three regions of cyclic hardening. An intermediate region, which is almost a flat plateau extending from 1.1×10^{-5} to 1.15×10^{-3}, is observed. The plateau-like region covers over three orders of plastic strain magnitude and the increase in saturation stress is only 12Mpa. The region can be defined as a quasi-plateau whose slope is much more flat comparing with those for the other two grain sizes. In region A and B, which correspond to lower and higher $\Delta\varepsilon_{pl}/2$ amplitude regions respectively, the saturation stress increases markedly with the increasing plastic strain amplitude.

4.3.3.2 Microstructure Observation

PSBs started to be observed in a sample which was tested at $\Delta\varepsilon_{pl}/2$ amplitude of 2.2×10^{-5},

Specimens	Frequency (Hz)	Total Strain	Plastic Strain	Saturation Stress (Mpa)
1	10	2.50E-4	5.30E-6	44
2	5	3.30E-4	1.10E-5	60
3	5	4.20E-4	2.20E-5	61
4	2.5	4.90E-4	2.80E-5	63
5	1.25	9.00E-4	2.20E-4	64.2
6	0.6	1.18E-3	4.60E-4	65.3
7	0.4	1.47E-3	7.10E-4	67
8	0.2	1.90E-3	1.15E-3	72
9	0.1	2.58E-3	1.66E-3	82
10	0.06	3.17E-3	2.00E-3	85
11	0.04	6.00E-3	4.22E-3	110
12	0.02	6.30E-3	5.22E-3	120

Table 4.8 Test conditions and cyclic response of 100μm-grained copper polycrystals cycled under constant strain control, with a low constant strain rate.

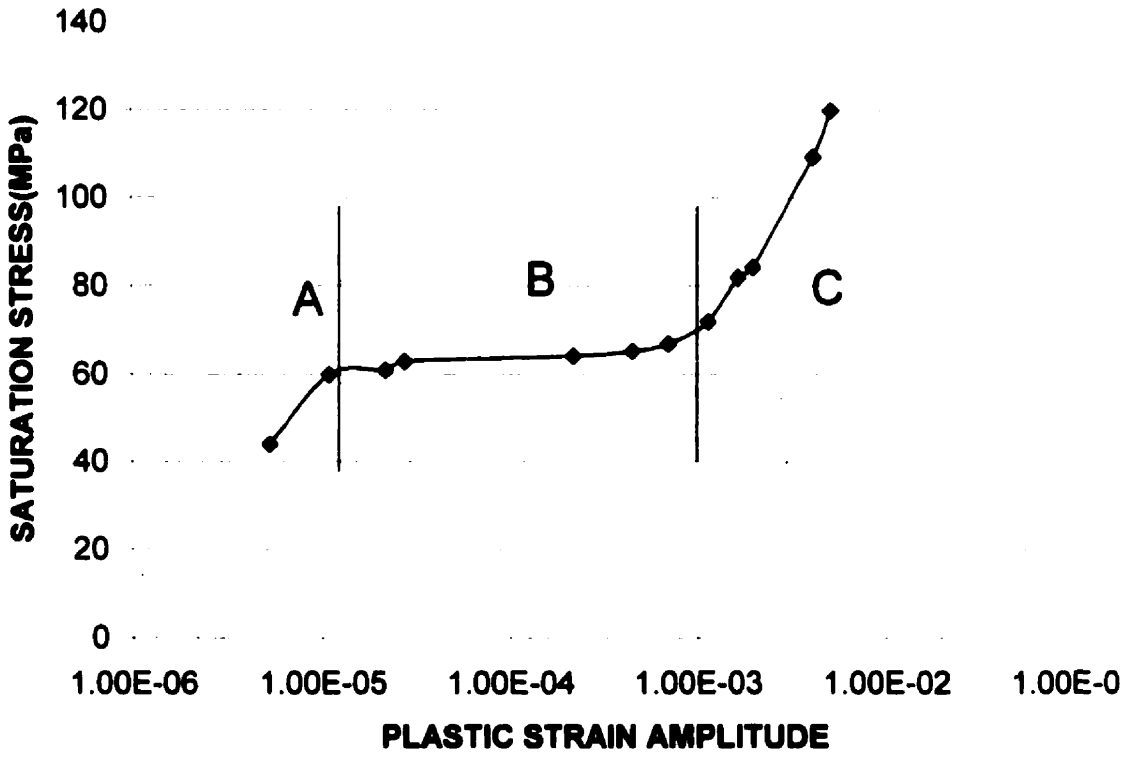

Figure 4.19 The CSS curve for 100μm-grained copper polycrystals

which is near to the lower end of the quasi-plateau, as shown in Figure 4.20. It can be seen that the picture shows a pair of PSBs, which were formed by breakdown of the surrounding matrix. Observation was further performed on higher $\Delta\varepsilon_{pl}/2$ amplitude alone the quasi-plateau region and it was found that PSB population increases with the increasing plastic strain amplitude and more than 30% grains contain ladder-like PSBs at the end of the quasi-plateau. It was observed that the formation of PSBs is much more pronounced in this coarse-grained polycrystals, comparing with that for 22μm- and 35μm-grained copper, where most of the grains contain one single or one pair of parallel PSBs. It was found that some grains were very favorable for very high localization of deformation and they contained high volume fraction of PSBs, some grains even were totally filled with PSBs as shown in Figure 4.21, which was taken for a sample tested at a $\Delta\varepsilon_{pl}/2$ amplitude of 7.1×10^{-4}. According to the investigation on the quasi-plateau region. SEM investigation on the samples in region C shows no significant increase of PSBs. However, evidence of second slip band was obtained. Figure 4.22 and 4.23 were taken for an etched sample corresponding to a $\Delta\varepsilon_{pl}/2$ amplitude of 4.22×10^{-3}. Figure 4.22 shows a secondary slips band at the grain boundary. Occasionally, intersection of secondary slip bands with PSBs was observed as shown in Figure 4.23.

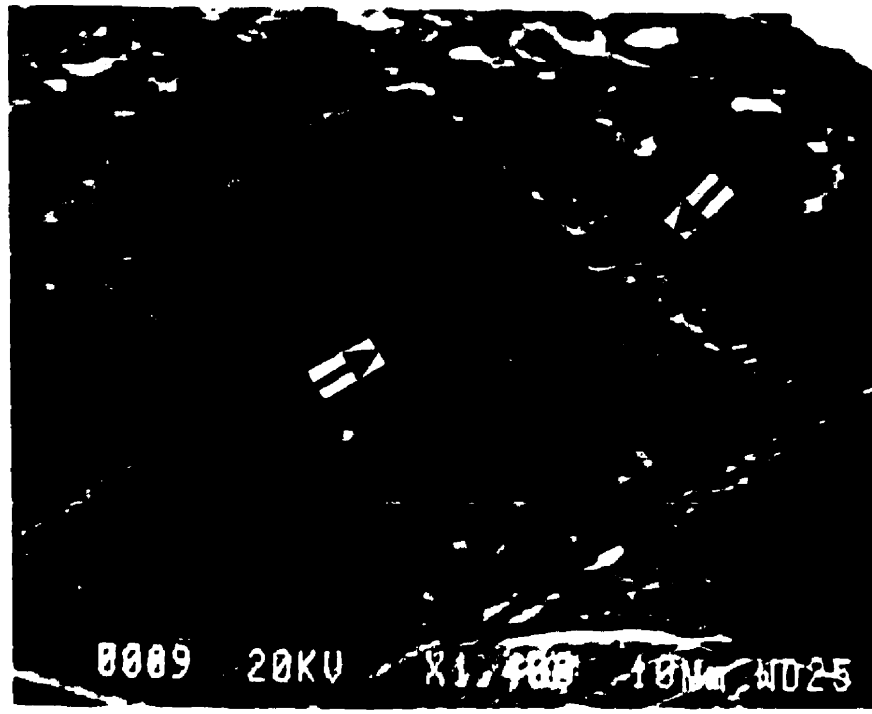

Figure 4.20 A pair of parallel PSBs in 100μm-grained sample tested at a plastic strain of 2.2×10^{-5}

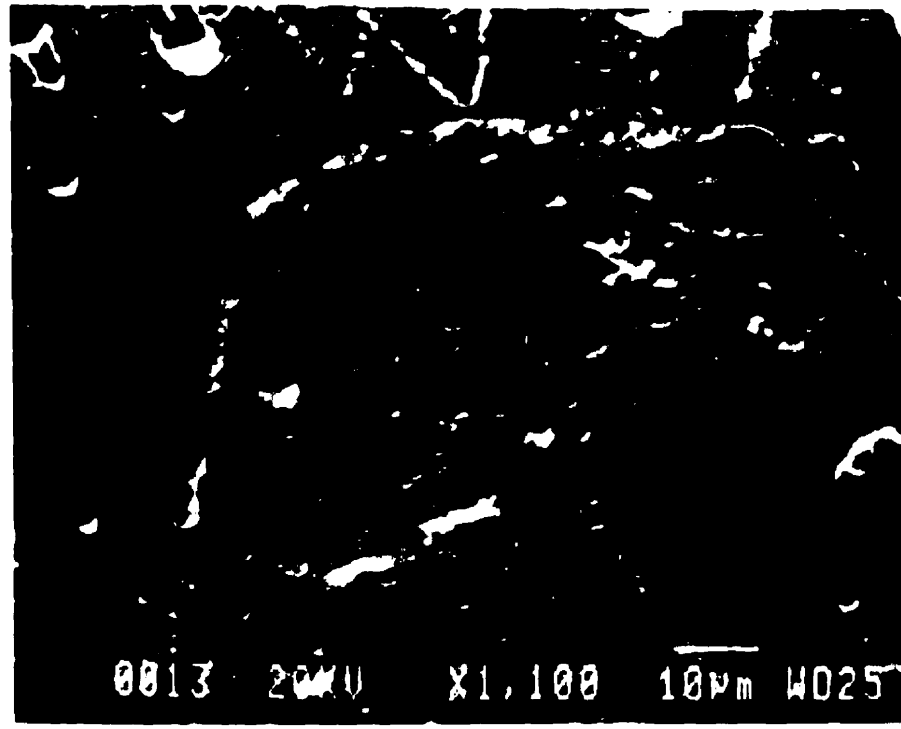

Figure 4.21 A grain fully filled with PSBs in 100μm-grained sample tested at a plastic strain of 7.1×10^{-4}

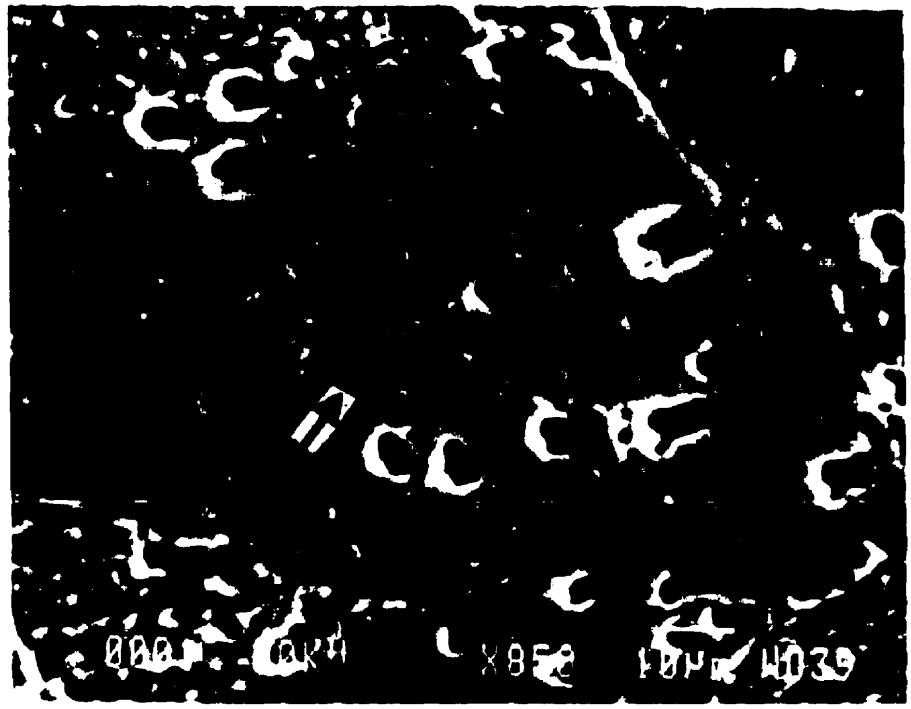

Figure 4.22 A secondary slip band in 100μm-grained sample tested at a plastic strain of 4.22×10^{-3}

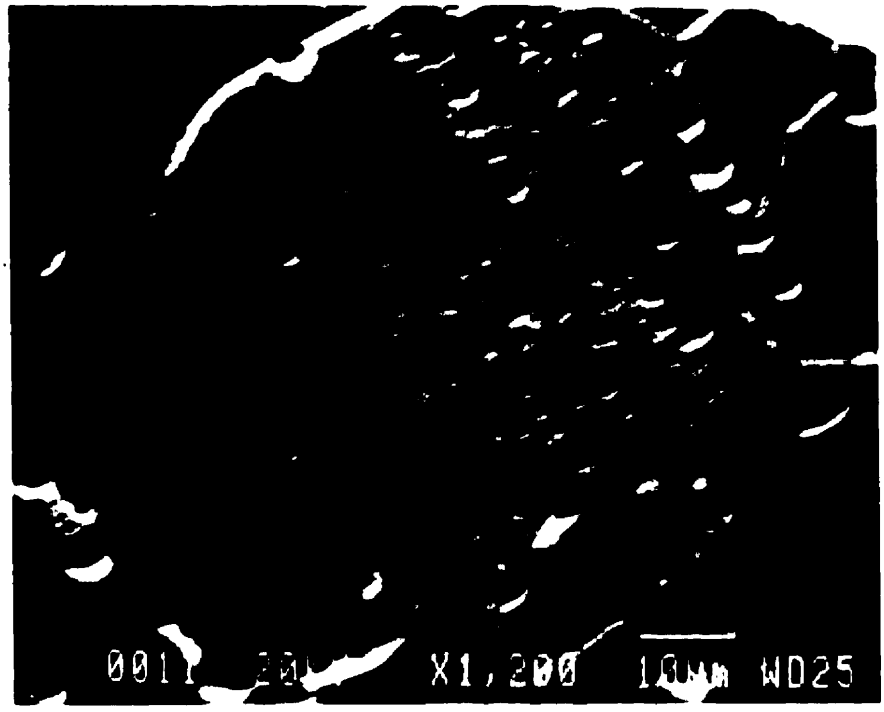

Figure 4.23 Intersection of secondary slip bands with PSBs in 100μm-grained sample tested at a plastic strain of 4.22×10^{-3}

4.4 COMPARISON OF CYCLIC BEHAVIOR OF COPPER POLYCRYSTALS WITH DIFFERENT GRAIN SIZE

4.4.1 The CSS Curves

The cyclic strain-stress curves for grain sizes of 22μm, 35μm and 100μm are compared as shown in Figure 4.24. In addition, the results by Liu and Bassim, whose study was conducted on 42μm- grained copper under the same testing conditions as the present test, are also provided for comparison.

It can be seen that all CSS curves exhibit three regions of cyclic hardening and a quasi-plateau region for each of the curves. However, a grain size effect on the curves was also noticed: 1) except at very low plastic strain range, a smaller-grained polycrystals clearly exhibits a higher saturation stress than that for a coarser-grained polycrystalline copper, 2) a finer-grained copper exhibits a steeper quasi-plateau than a coarser-grained copper 3) the quasi-plateau region for a finer-grained copper starts earlier and ends latter, comparing with that for a coarser-grained polycrystals.

The quantitative description of above-mentioned aspects is provided in Table 4.9. The extension of a quasi-plateau region is given in terms of plastic strain amplitude for the onset to the end of the region. A fatigue limit is defined as a saturation stress and the corresponding plastic strain amplitude below which a PSB is absent; because no PSB formed just below the onset of a quasi-plateau, the onset of the region is given for this

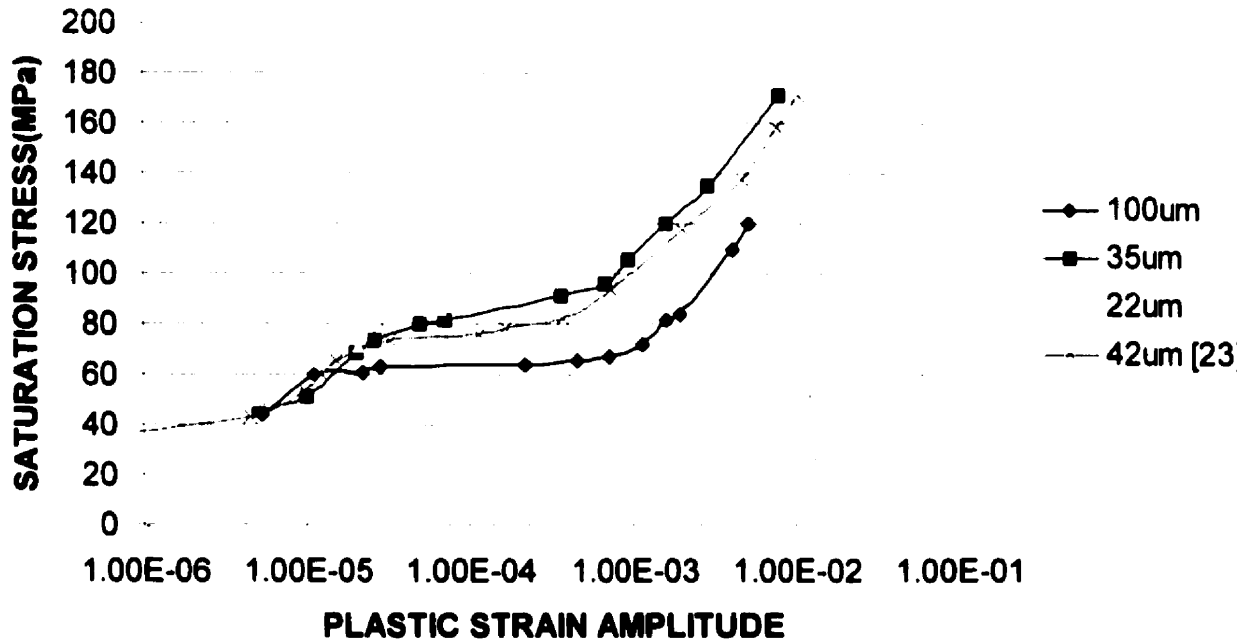

Figure 4.24 Comparison of the CSS curves from the present and Liu's study [23]

Grain Size (μm)	Extension of the Quasi-plateau	Fatigue Limit (MPa)	Effective Orientation Factor M	Slope of the Quasi-plateau (Mpa/order of $\Delta\varepsilon_{pl}/2$)
22	3.2×10^{-5}-3.75×10^{-4}	81	2.89	21
35	2.6×10^{-5}-6.8×10^{-4}	74	2.64	16
42	1.5×10^{-5}-7.4×10^{-4}	72	2.59	14
100	1.1×10^{-5}-1.66×10^{-3}	61	2.18	6

Table 4.9 Aspects of differences of the CSS curves for different grain size

factor. The effective orientation factor M is given as the ratio between a fatigue limit for polycrystalline copper and that for the single crystal (28MPa) [8], it is found that a M is larger for a smaller-grained copper polycrystals than that for a coarser-grained copper. The unit of the slope of a quasi-plateau is defined as change of saturation stress per order of plastic strain magnitude. The data provided shows that the slope of a quasi-plateau is steeper for a finer-grained polycrystal than that for a coarser one.

4.4.2 Comparison of the Microstructures

The present SEM investigation shows that 1) in region A, there are no PSBs or secondary slip bands observed. 2) in region B, PSBs start to form at the lower ends of the quasi-plateaus. In general, the PSB population increases with the applied $\Delta\varepsilon_{pl}/2$. However, the increase in the population for smaller –grained copper is not as fast as that for a coarser-grained copper. At a end of a quasi-plateau, less than 8% grains contain PSBs in 22μm-grained material, around 12% grains contain PSBs in 35μm-grained copper, while for 100μm-grained polycrystals, more than 30% grains contain PSBs. Another important information, which was obtained from the SEM investigation and should be mentioned, is that the PSBs in fine grain copper distribute more randomly comparing with that in 100um-grain copper. Most of the grain containing PSBs was fully filled with them, while in 22μm-grain copper most of them contain only one or two clusters of PSBs.

CHAPTER 5 DISCUSSION

The results described in the previous chapter show clearly the grain size effect. This chapter provides a discussion to correlate the mechanical response with the microstructural observation.

5.1 GRAIN SIZE EFFECT ON CSS RESPONSE

As mentioned in the literature review, a true plateau in CSS response of copper single crystal is well established, but studies on polycrystalline copper show a significant scatter. A controversy over whether or not there exists a plateau has been argued for many years.

The present studies on different-grained polycrystalline copper reveal three regions of cyclic hardening. In region A and region C, which correspond to low and high plastic strain region respectively, saturation stress increases markedly with increasing plastic strain. In region B, which corresponds to intermediate plastic strain region, a quasi-plateau is observed. The occurrence of quasi-plateau region in CSS curve of polycrystalline copper was reported in the literature [18, 19, 23, 32]. Liu [23, 32] claimed a quasi-plateau region in the CSS curve of 42μm-grained copper. The result obtained through his study is comparable with the currently obtained CSS curves, which must be due to the same testing conditions.

Mugrabi [19] does not claim a quasi-plateau in his investigation on 25μm-grained copper. However, it can be seen from the CSS curve obtained from his study that within the plastic strain below 10^{-2}, which is the range the current tested being conducted, shows three regions of cyclic hardening instead of four regions; and a clear quasi-plateau exist in the intermediate region II.

A recent study by Mayer and Laird [38] shows that testing frequency significantly influences the cyclic behavior of copper ploycrystals. They found that low cyclic frequency stimulates PSB transformation from loop patches. In other word, low cyclic frequency promotes localization of deformation. Since it is well-known that the formation of PSB influences cyclic response by reducing the slope of cyclic hardening and both present study and above mentioned studies were performed under low frequency, thus it is not surprising that a quasi-plateau exists, in other word, the studies are mutually supported. Moreover, those studies, which result in a true plateau [8,17] were also using low testing frequencies.

Reviewing the CSS curves of copper polycrystals published in the literature, the test conditions can be classified into two broad categories of low constant strain rate ($<10^{-2}$/s) and high constant frequency (>10Hz). The plateau-like behavior was more pronounced when the test was performed under low strain rate, while the CSS curves of polycrystals tested at constant high frequency show less plateau behavior or even no plateau behavior [26-28, 33, 37].

Grain size effect on cyclic response was conducted on 22μm-, 35μm- and 100μm-grained copper polycrystals in the present study. As can be seen from Fig. 4.9: a fine-grained copper clearly exhibits a higher $\Delta\sigma_s/2$ than a coarse-grained copper except at very low $\Delta\varepsilon_{pl}/2$. The extension of quasi-plateau reveals grain size effect as well: the coarser the grain size, the longer the extension of the plateau. In addition, the quasi-plateau region shows a different slope for a different grain size.

It is well known that the effects of grain size on monotonic deformation are described through models such as the Hall-Petch relation. This effect is due to the influence of grain size on the limiting slip length, dislocation density and dislocation pile-ups [70,71]. In general, it is indicated that flow stress is proportional to the square root of dislocation density and that dislocation density is inversely proportional to slip length. At low strain the dislocation slip length approaches the dimension of the grain. Therefore, as grain size decreases, the flow stress increases. As was demonstrated for copper in this study, persistent slip bands nucleated in the grain boundary and extended toward the opposite side of GB, most of them reached the other side of the GB. So it is reasonable that a small-grained copper reveals higher $\Delta\sigma_s/2$ value. At higher $\Delta\varepsilon_{pl}/2$, where dislocation structures such as cells form, the slip length approaches the cell dimension. If the effect of GS has little influence on cell diameter, the effect of GS on flow stress is negligible. It has been reported that the GS effect in monotonically deformed copper diminishes or even reverse at high strains [70].

Several investigators [24, 27, 68, 69] reported typical effect of grain size on cyclic response of copper polycrystals. It is known that the relatively open vein structure is formed at low $\Delta\varepsilon_{pl}/2$, so slip length may be a function of grain diameter, which means grain size may be expected to influence saturation behavior. However, at very high $\Delta\varepsilon_{pl}/2$ amplitude a well-defined cell structures forms. Since grain size does not show the influence on cell size, grain size would not be expected to influence saturation behavior at very high amplitude. This behavior in cyclically deformed copper was reported by Johnston and Feltner [71]. The results of the present study generally reflect the typical behavior, namely, higher $\Delta\sigma_s/2$ for smaller grain size. However, at very low $\Delta\varepsilon_{pl}/2$, grain size effect on $\Delta\sigma_s/2$ is not well defined. This may be attributed to the mechanical error or other explanations, which are left open for future study. It should be mentioned that the present LCF was not performed up to very high $\Delta\varepsilon_{pl}/2$ amplitude, where cell structure is well developed. However, it can be clearly seen that the ends of the CSS curves are approaching each other which gives a hint that they might intercept at higher $\Delta\varepsilon_{pl}/2$, where cell structure is well developed.

As demonstrated in Fig. 4.9 and Table 4.10, the extension of the quasi-plateaus shows grain size effect, where the quasi-plateau started earlier and ended latter for a coarser grain size comparing with that for finer grain size. As will be described in next subsection, the onset of a quasi-plateau indicates the formation of PSBs by breaking down vein structure, and the end of a quasi-plateau indicates the saturation of PSB formation, and secondary slip band starts to occur as a consequence of further application of $\Delta\varepsilon_{pl}/2$.

To analyze the obtained results, a realistic model of polycrystalline behavior in cyclic deformation has been attempted. Here, a qualitative model of the behavior of polycrystalline material is presented for which the results obtained for the present study can be used as a test. The description of the grain, which is considered to be the grain modeling approach, was proposed initially by Hirth [72]. In his study, a single deforming grain was proposed to be composed of one hard region near the grain boundary and a soft region corresponding to the interior of the grain, as shown schematically in Fig. 5.1. The hard region is caused by multiple slip produced by plastic incompatibilities from adjacent grains and thus, it enhances homogenization of deformation until the whole grain becomes hard. The soft region has a single slip character at low and intermediate strain amplitudes, so it is associated with localization of deformation by forming PSBs in cyclic deformation.

Bassim and Liu [64], based on their TEM study on cyclic saturated polycrystalline copper with 42um grain size, concluded 1) in region A, cylindrical loop patch structure which was observed in single crystals and coarse-grained polycrystals was also formed in 42um-grained copper, moreover, the irregular loop patch and cellular loop patch, which were rarely reported to occur in the coarse-grained copper and single crystals, were observed in region A for 42um-grained copper. 2) In region B for 42μm grain size, the dislocation structure formed veins, PSBs structure were also present in this region, but with much lower fraction than that found in the coarse grain size and copper single crystals reported in the literature.

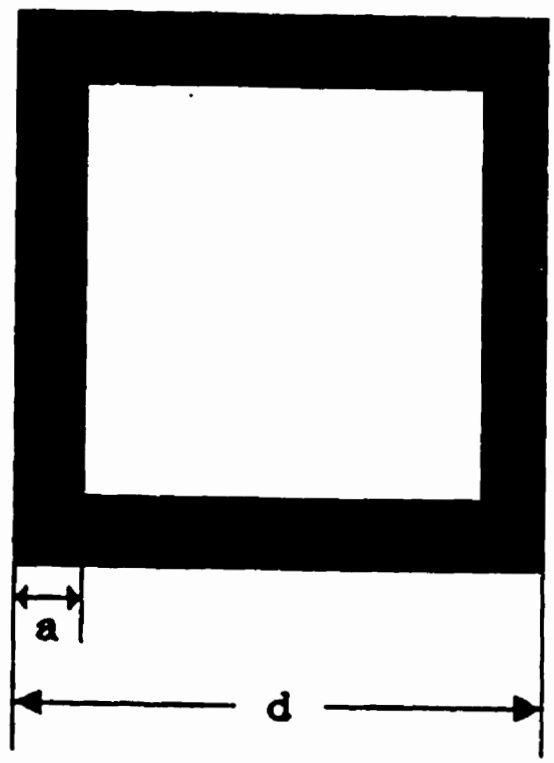

Figure 5.1 Schematic representation of a grain, from Ref. [72]

Both of the above mentioned studies indicate that the smaller the grain size, the more pronounced multiple slip behavior, which leads to more homogeneous deformation. The presently obtained results can be explained exactly in the same way. Since a coarse grain can be intimately correlated to a bigger volume fraction of soft region oriented for single slip at which PSBs are more promoted to form than that for a smaller grain. On the other hand, a small grain has larger volume fraction of hard region oriented for multiple slip, which promote more homogenous deformation and constraint effect is more significant because of compatibility requirement, and thus the applied deformation can be distributed among the whole grains more effectively. Therefore, formation of PSB, which indicates the start of the quasi-plateau, might need larger $\Delta\varepsilon_{pl}/2$ and $\Delta\sigma_s/2$ to be applied for a small grained polycrystals.

For coarse-grained polycrystals, constraint effect from the adjacent grains is less significant because the volume fraction of the hard region is small compared with that for a smaller grain. It is more favorable for localization of deformation than for homogeneity of deformation. For a small grain the effect is opposite: compatibility requirement is more pronounced, the localization of deformation could be suppressed easily because of significant constraint effect caused by higher density of grain boundaries, which promotes multiple slip behavior.

5.2 GRAIN SIZE EFFECT ON PSB FORMATION

As demonstrated in chapter 4, PSBs formed during the cyclic deformation. All the PSBs on the polycrystalline copper show short and straight thin lines, which were broken down from the surrounding matrix. They nucleated at a grain boundary without directly crossing it. Occasionally, it may be observed that PSBs in two adjacent grains intersect each other and run along a different direction. These common features, which were also observed by Liu [23, 64], indicate that grain boundaries play an important role on the formation of PSBs.

5.2.1 PSBs in Fine-Grained Copper Polycrystals

The investigation on smaller-grained polycrystals (22μm and 35μm) shows that PSB population increases with increasing $\Delta\varepsilon_{pl}/2$ amplitude along the quasi-plateau region. However, even at the ends of the quasi-plateau regions there are only less than 10% grains containing this ladder-like structure. The PSBs formed in small-grained polycrystals are randomly distributed in the bulk of the polycrystals. The results obtained from the present study support Bassim and Liu's investigation on 42μm-grained copper [23, 64].

Liu and Bassim [23] concluded, based on their study, that PSBs is not the governing microstructure in fine-grained copper polycrystals. Since only few grains can just orient with the primary slip system, which are favorable to build up the ladder-like PSBs, the major contribution to the saturation stress is from the deformation of the bulk matrix. When the vein structure of the matrix breaks down and forms PSBs in some grains, it

reduces the stress sustained by these grains. However, the decrease of the stress on the grains leads to the redistribution of stresses among all grains and results in a stress rise in the neighboring grains. Therefore, due to the high constraint of small grain size, localization of deformation is not easy to observe and the matrix receives most of applied $\Delta\varepsilon_{pl}/2$.

Liu asserted that the description in term of a two phase model, which regard the PSB structure as the soft phase determining the saturation stress on the bulk of material [54], is not applicable in polycrystals. He made an assumption that the PSBs can be considered to mix up with the matrix in the manner of a composite, the saturation stress on the bulk of a polycrystals may be assumed as obeying a mixture law. He proposed a model according to the assumption:

$$\Delta\sigma_s/2 = M\ (f_m\tau_m + f_{PSB}\tau_{PSB})$$

where $\Delta\sigma_s/2$ = axial saturation stress in polycrystals

M = effective orientation factor

f_m = volume fraction of matrix structure

f_{PSB} = volume fraction of PSB structure

τ_m = shear stress in matrix structure

τ_{PSB} = shear stress in PSB structure

The currently obtained CSS curves of 22μm- and 35μm-grained copper, which can treated as fine-grained materials, show quasi-plateau regions. The microstructure observation shows that amount of PSBs is very small even at the upper end of the quasi-plateaus, so the saturation stress is mainly contributed by a combination of matrix structure and PSB structure.

Moreover, the quasi-plateau region for 22μm-grained copper is steeper than that for 35μm-grained copper. This can be explained by the above-mentioned composite model in terms of volume fraction of PSBs, which is bigger for 35μm-grained copper than that for 22μm-grained material.

5.2.2 PSBs in Coarse-Grained Polycrystals

A very flat quasi-plateau was observed in the CSS curve of 100μm-grained copper. The SEM observation shows PSB population increases linearly with applying $\Delta\varepsilon_{pl}/2$ along the quasi-plateau, and up to approximately 30% grains contain this ladder-like PSBs at the end of the quasi-plateau. Moreover, some of them are almost full-filled with PSB structure.

A true plateau behavior is well-known to be observed in CSS curve for copper single crystal [8]. The onset of the plateau is marked by the formation of PSBs; the PSB density increases linearly as the strain amplitude increases, and at the end of the plateau the entire crystal was occupied by PSBs. It was found the flow stress of the cycled crystal depended

on the stress sustained by the PSBs, which means that PSBs are responsible and dominant for the plateau behavior. Based on the investigation, a model describing the cyclic behavior of copper single crystal was proposed, which is called two-phase model [8, 16]:

$$\Delta\gamma_{pl}/2 = f_{PSB}(e_b - e_m) + e_m$$

where f_{PSB} is the volume fraction of the PSBs, e_b is the local plastic shear strain amplitude in the ladder structure, e_m is the local plastic shear strain amplitude in the matrix structure, $\Delta\gamma_{pl}/2$ is the plastic shear strain amplitude applied.

The structure and properties of the two phases are found generally to be independent of the platic shear strain amplitude. The law of mixtures shows the linear relationship between f_{PSB} and $\Delta\gamma_{pl}/2$ found for the single crystals. It also explains the constant saturation stress in the plateau between the value e_b and e_m of $\Delta\gamma_{pl}/2$. For single crystals, the two-phase model explains the plateau: the τ_{PSB} in the plateau is the flow stress of the unconstrained wall structure at its local plastic strain.

True plateau behavior of polycrystalline copper was also reported by several investigators [14, 15, 17, 20, 22, 25]. Pedersen *et al.* [17], who got a plateau region in the study on 150um-grained polycrystals, found that more than 60% grains contained PSBs at plastic strain amplitude near to the upper end of the plateau. They suggested that the dislocation microstructure in coarse-grained polycrystals was qualitatively similar to that in single crystals. The PSB pattern shows a similar tendency for individual grains to avoid PSB on

more than one slip system, which indicates the plastic strain is carried mainly by PSBs with single slip.

The explanation of occurrence of plateau region was given by Wang [73], who studied copper bicrystal. Based on TEM investigation, he found that the grain boundary acted as an obstacle to the motion of dislocations and at the end of the plateau region. a secondary slip system was activated. However, the population of the PSBs increases linearly and rapidly along the plateau. Actually, the phenomenon that activation of secondary slip systems at the end of the plateau was also observed in single crystal studied by Mugrabi [8]. Therefore, we can safely state that as long as the PSBs is predominant, the occurrence of a plateau should be possible in the CSS curve.

The present study on 100μm-grained copper shows a very horizontal quasi-plateau, where the $\Delta\sigma_s/2$ increase very slow with increasing $\Delta\varepsilon_{pl}/2$, comparing to that for 22μm- and 35μm-grained materials. The composite model is reasonable for explaining the behavior of current fine grain copper, where combination of matrix structure and PSBs control the saturation stress. However, for coarse-grained copper, the contribution of PSBs to the saturation stress is larger, and they play a more important role in cyclic response.

Since the composite model explains the quasi-plateau behavior, while the two-phase model explains the plateau behavior in terms of PSB formation, we can safely state, based on the present study, that the composite model is reasonable for explaining CSS

behavior of polycrystalline material. However, when the grain size gets significantly larger, the mechanism of fatigue would be in the way of approaching the two-phase model, especially for extremely large grain size. This is supported by Kuokula's study [20], where copper polycrystals with a grain size of 2mm was used.

5.3 Grain Size Effect on Fatigue Limit

The role of PSB on the initiation of fatigue cracks in metals, especially in the low amplitude region, has long been recognized [52, 66]. Th existence of threshold amplitude below which no PSBs were formed provides an indication of fatigue limit. Based on the present study as well as previous studies in the literature, a sign of slope reduction in CSSC reflects the occurrence of PSBs. Therefore, determination of a fatigue limit value is straightforward.

In the present study, cyclic response for different grain size reveals different fatigue limits, which are 61Mpa, 75Mpa or 81Mpa for 100μm-, 35μm- or 22μm-grained copper, respectively. It is established that the fatigue limit in single crystals is at a threshold value of 28Mpa, which corresponds to the beginning of the plateau, where PSBs start to form. To correlate the fatigue limit for polycrystals to that for a single crystal, an average orientation factor was obtained, which is 2.18 for 100μm-grained copper, 2.64 for 35μm grain size and 2.89 for 22μm grain size as shown in Table 4.9 in chapter 4.

In the literature. Pedersen [24] reported a Sachs factor of 2.24 as an effective correlation factor between the fatigue limit for 150μm-grained copper and that for single crystal, which is 28Mpa. This is in conjunction with the fatigue behavior obtained by him, because Sachs factor assumes that the material is deformed by single slip.

Conventionally, the Sachs factor is considered to be an effective orientation factor for cyclic deformation of polycrystalline materials since single slip takes the major role at low plastic strain. However, when grain size is small, the compatibility requirement promotes multiple slip even at low $\Delta\varepsilon_{pl}/2$ amplitude.

Liu and Bassim found that even in region A, which corresponds to very low $\Delta\varepsilon_{pl}/2$, irregular loop patches formed indicating the activation of multiple slip system. A fatigue limit of 72Mpa is obtained, from which an effective factor of 2.59 was calculated.

Employment of Taylor factor (3.06), which assumes that the material is mainly deformed by multiple slip, was reported by Wang [32]. The fact that such a high $\Delta\sigma_s/2$ was obtained is due to their unique method of testing: ramp load, which produces a more uniform dislocation loop structure than conventional testing method. The pre-treated microstructure promotes a homogenous PSB formation with a higher flow stress. Therefore, the result represents an upper bound of fatigue limit.

The convention idea of treating Sachs factor as low bound of conversion, while Taylor factor as upper bound was broadened by Liu [23] due to the fact that the polycrystalline

copper consists of the grains with arbitrary orientation where the maximum Schmid factor is 0.5 for [1, -9.9, -4.45] orientation and minimum Schmid factor is o.272 for [112] orientation. Therefore, the correlation factor can be obtained by inverting the two extreme Schmid factors, which are 2 and 3.68, respectively.

The present study shows that the smaller the grain size, the higher the fatigue limit and effective orientation factor. This is consistent with the premise that a coarse grain is more likely to be deformed by single slip, whereas multiple slip plays a more important role in the deformation of fine-grained material.

CHAPTER 6 CONCLUSIONS

The cyclic response and the formation of the PSBs in copper polycrystals of various grain sizes have been investigated. On the basis of the experimental results, the following conclusions can be drawn:

1. All the CSS curves of the copper polycrystals with different grain size exhibit three regions of cyclic hardening, in which a quasi-plateau region occurs where the saturation stress increases less significantly with increasing plastic strain amplitude than that for the region A and the region C.

2. In general, a finer-grained copper shows a higher saturation stress. The difference in saturation stress is primarily caused by higher back stresses in the finer-grained material. However, this trend is undefined in the very low plastic strain region. A tendency that the ends of the CSS curves are approaching each other indicates that grain size might lose its effect at higher plastic strain.

3. The quasi-plateau regions show grain size effect in that: (a) the larger the grain size, the earlier the beginning and the latter the ending of the quasi-plateau, in terms of plastic strain and (b) the smaller the grain size, the steeper the quasi-plateau.

4. SEM investigation shows that grain size influences the slip character of the material. The PSBs occur at lower plastic strain amplitude and the secondary slip bands occur at higher plastic strain amplitude in a coarser-grained copper.

5. The fact that a PSB occurs at higher plastic stain amplitude and saturation stress indicates a greater fatigue limit for fine-grained copper polycrystals.

REFERENCES

1. M. Klesnil and P, Lukas. *Materials Science Monographs*, 7. (1980).
2. A. T. Winter, *Phil. Mag.* **30**, 719 (1974).
3. B. D. Yan, A. S. Cheng, L. Buchinger, S. Stanzl and C. Laird, *Mater. Sci. Engng.* **80**, 129 (1986).
4. A. S. Cheng, L. Buchinger, S. Stanzl and C. Laird, *Mater. Sci. Engng.* **80**, 155 (1986).
5. S. Horibe and C. Laird, *Acta metall.* **31**, 1567 (1983).
6. S. Horibe and C. Laird, *Sci. Engng.* **72**, 149 (1985).
7. S. Horibe and C. Laird, *Acta metall.* **35**, 1919 (1987).
8. H. Mughrabi, *Mater. Sci. Engng.* **33**, 207 (1978)
9. P. T. Wood, *Phil. Mag.* **28**, 155 (1973).
10. L. Buchinger, S. Stanzl and C. Laird, *Phil. Mag.* **A**, 50 (1984)
11. T. H. Alden and W. A. Backofen, *Acta metall.* **9**, 352 (1961).
12. W. N. Roberts, *Phil. Mag.* **20**, 675 (1969).
13. J. M. Finney and C. Laird, *Phil. Mag.* **31**, 339 (1975).
14. D. Kuhlmann-Wilsdorf and C. Laird, *Mater. Sci. Engng.* **27**, 137 (1977)
15. D. E. Witmer, G. C. Farrington and C. Laird, *Acta metall.* **35**, 1895 (1987).
16. P. Lukas and M. Klesnil, *Mater. Sci. Engng* **11**, 34 (1973)
17. K. C. Rasmussen and O. B. Pederson, *Acta metall.* **28**, 1467 (1980).
18. J. C. Figueroa, S. P. Bhat, R. De La Veaux, S. Murzenski and C. Laird, *Acta metall.* **29**, 1667 (1981).

19. H.Mughrabi and R. Wang, *Mechanisms and Microstructures, Proc 2ndRisφ Int. Symp. On Metallurgy and Materials Science*, p. 89. (1981)

20. V.-J. Kuokkala, T. Lepisto and P. Kettunen, *Scripta metall.* **16**, 1149 (1982)

21. A. T. Winter, O. B. Pedersen and K. V. Rasmussen, *Acta metall.***29**, 735 (1981)

22. Z. S. Basinski and S. J. Basinski, *Acta metall.* **37**, 3255 (1989)

23. C. D. Liu, M. N. Bassim and D. X. You, *Acta metall.* **42**, 1631 (1994)

24. O. B. Pedersen, *Acta metall.* **38**, 1221 (1980)

25. O. B. Pedersen and K. V. Rasmussen, *Acta metall.* **30**, 57(1982)

26. J. Polak and M. Klesnil, *Mater. Sci. Engng.* **63**, 189 (1984)

27. H. Mulliner, B. Weiss, R. Stickler, P. Lukas and L. Kunz, *Fatigue 84, Proc. 2nd Int. Conf. On Fatigue and Fatigue Thresholds.* Vol. 1, 423. (1984)

28. P. Lukas and L. Kunz, *Mater. Sci. Engng.* **85**, 67 (1987)

29. P. Lukas and L. Kunz, *Mater. Sci. Engng.* **A103**, 233 (1988)

30. C. D. Liu, and M. N. Bassim, *Phys. Stat. Sol.* (a)**149**, 323 (1995)

31. C. D. Liu, and M. N. Bassim, *Phys. Stat. Sol.* (a)**149**, 331(1995)

32. C. D. Liu, and M. N. Bassim, *The Japan Institute of Metal*, P. 473 (1994)

33. L. Llanes and C. Laird, *Mater. Sci. Engng.* **A128**, L9 (1990)

34. L. Llanes, A. D. Rollett, J. L. Bassani and C. Laird, *Acta metall* **41**, 2667 (1993)

35. L. Llanes and C. Laird, *Mater. Sci. Engng.* **A161**, 1 (1993)

36. L. Llanes, J. L. Bassani and C. Laird, *Acta metall* **42**, 1279 (1994)

37. Z. Wang and C. Laird, *Acta metall* **100**, 57 (1988)

38. H. Mayer and C. Laird, *Mater. Sci. Engng.* **A187**, 23 (1994)

39. J. Polak, K. Obrtlik and J. Helesic, *Mater. Sci. Engng.* **A132**, 67 (1991)

40. P. Neumann, and P. Hassen, "Physical Metallurgy",Elsevier, New York, 1553 (1983)

41. P. Neumann, *Metallkd.* **59**, 927 (1968)

42. B. Yan, A. Hunsche, P. Neumann and C. Laird, *Mater. Sci. Engng.* **79**, 9 (1986)

43. B. Yan and C. Laird, *Mater. Sci. Engng.* **80**, 59 (1986)

44. A. W. Thompson and W. A. Backofen, Acta Metall. **19**, 597 (1971)

45. R. W. Armstrong, Metall. Trans.**1**, 1169 (1970)

46. H. Mughrabi and R. Wang, "*Basic Mechanisms in Fatigue of Metal*", Proc. of the Int. Coll. "Basic Mechanisms in Fatigue of Metal" , Elsevier, Brno, 83 (1988)

47. H. J. Christ, H. Mughrabi and C. Wittig-Link, "*Basic Mechanisms in Fatigue of Metal*", Proc. of the Int. Coll. "Basic Mechanisms in Fatigue of Metal" , Elsevier, Brno, 83 (1988)

48. J. Boutin, N. Marchand, J. P. Bailon and J. I. Dickson, *Mater. Sci. Engng.* **67**, L23 (1984)

49. D. J. Morrison, *Mater. Sci. Engng.* **A187**, 11 (1994)

50. C. Larid and L. Buchinger, *Metall. Trans.* **A16**, 2201 (1985)

51. N. Thompson and N. Wadsworth, *Phil. Mag.* **7**, 223 (1954)

52. N. Thompson, N. Louat and N. Wadsworth, *Phil. Mag.* **1**, 113 (1956)

53. L. M. Brown, Metals Sci. **11**, 315 (1977)

54. N. Thompson, N. Louat and N. Wadsworth, *Phil. Mag.* **1**, 113 (1956)

55. C. Laird, *Mater. Sci. Engng.* **22**, 231 (1976)

56. G. I. Taylor, Inst. Met. **62**, 307 (1938)

57. H. Mecking, V. Gerold and G. Kostorz, "*Strength of Metals and Alloys*", Proc. ICSMA 5, Pergamon Press, Oxford, **Vol.3**, 1573 (1980)

58. U. F. Kocks, *Metall. Trans.* **1**, 1121 (1970)

59. G. Z. Sachs, *Verein. Dt. Ing.* **72**, 734 (1929)

60. J. D. Eshelby, *Proc. Roy. Soc.*, **A241**, 376 (1957)

61. O. B. Pedersen, K. V. Rasmussen and A. T. Winter, *Acta Metall.* **30**, 57 (1982)

62. U. F. Kocks and G. R. Canova, in N. Hansen, A. Horsewell, T. Leffers and H. Lilhot (eds.), *Deformation of Polycrystals*, Riso National Laboratory, Roskilde, Denmark. 35 (1981)

63. T. Leffers, in N. Hansen, A. Horsewell, T. Leffers and H. Lilhot (eds.), *Deformation of Polycrystals*, Riso National Laboratory, Roskilde, Denmark, 55 (1981)

64. M. N. Bassim, C. D. Liu and D. X. You, *Acta metall.* **42**, 3695 (1994)

65. E. Kroner, *Acta metall.* **9**, 155 (1961)

66. American Society for Metals, *Metals Handbook Desk Edition*, **8**, 7.15 (1985)

67. D. Kuhlmann-Wilsdorf and C. Laird, *Mater. Sci. Engng.* **50**, 209 (1980)

68. D. J. Morrison, V. Chopra and J. W. Jones, *Scripta. Metall.* **25**, 1299 (1991)

69. J. Boutin, N. Marchand, J. P. Bailon and J. I. Dickson, *Mater. Sci. Engng.* **67**, L23 (1984)

70. A. W. Thompson, M. I. Baskes and W. F. Flanagan, *Acta metall.* **21**, 1017 (1973)

71. T. L. Johnston and C. E. Feltner, *Metall. Trans.* **1**, 1161 (1970)

72. Hirth, *Metall. Trans.* **3**, 3047 (1972)

73. Y. M. Hu, Z. G. Wang and G. Y. Li, *Mater. Sci. Engng.* **A208**, 260, (1996)